The Pennsylvania State University

The Graduate School

Department of Mechanical and Nuclear Engineering

ACTIVE CONTROL OF STRUCTURAL VIBRATION AND ACOUSTIC RADIATION VIA LEFT AND RIGHT EIGENVECTOR ASSIGNMENT

A Thesis in

Mechanical Engineering

by

Tian-Yau Wu

Submitted in Partial Fulfillment
of the Requirements
for the Degree of

Doctor of Philosophy

May 2007

The thesis of Tian-Yau Wu was reviewed and approved* by the following:

Kon-Well Wang
William E. Diefenderfer Chaired Professor in Mechanical Engineering
Thesis Advisor
Chair of Committee

Chris D. Rahn
Professor of Mechanical Engineering

Mary Frecker
Associate Professor of Mechanical Engineering

Heath Hofmann
Associate Professor of Electrical Engineering

Karen A. Thole
Professor of Mechanical Engineering
Head of the Department of Mechanical and Nuclear Engineering

*Signatures are on file in the Graduate School

ABSTRACT

The goal of this thesis research is to investigate the feasibility of utilizing the left and right eigenvector assignment concept for active control of structural vibration and acoustic radiation.

The right eigenvector assignment approach is directly related to mode shape tailoring. It therefore can be utilized to achieve structural vibration confinement and acoustic radiation reduction. The control strategy of vibration confinement is to alter the right eigenvectors through active action, such that the modal components corresponding to the concerned region have relatively small amplitude. Similarly, the control strategy for reducing acoustic radiation is to alter the right eigenvectors through active action so that the modal velocity distributions cause as small radiation as possible. Reciprocally, the concept of left eigenvector assignment is to alter the left eigenvectors so that the effects of the exogenous disturbances on the system responses can be modified. Therefore the left eigenvector assignment can be conceptually used to reduce the effects of external excitations, and thus achieve disturbance rejection. The design goal is to alter the left eigenvectors through active action such that the forcing vectors are as closely orthogonal to the left eigenvectors as possible. Because of these clear physical meanings, the proposed left-right eigenvector assignment concept can target the nature of the structural vibration-acoustics problem with more physical insight as compared to many more classical control schemes. With such an approach, one can achieve both disturbance rejection and modal confinement (vibration control purpose) or modal

radiation reduction (noise reduction purpose) concurrently for forced vibration-acoustics problems.

In this research, simultaneous left-right eigenvector assignment and partial left-right eigenvector assignment approaches are synthesized for structural vibration control (discussed in Chapters 2 and 3 of this thesis) and acoustic radiation reduction (Chapter 5), respectively. With the simultaneous left-right eigenvector assignment approach, the feedback gain matrix is derived based on the generalized inverse procedure. In such a method, all the left and right eigenvectors of the closed-loop system are determined to best-match the desired eigenvectors through a least square approximation. On the other hand, the partial left-right eigenvector assignment method can exactly assign the selected left and right eigenvectors of the closed-loop system as the desired optimal ones. With this algorithm, both the left and right eigenvectors can be determined accurately from the achievable subspaces through solving generalized eigenvalue problems.

Numerical simulations are performed to evaluate the effectiveness of the proposed methods on a clamped-clamped beam structure example for the vibration and noise control problem. Frequency responses of different case studies in the selected frequency range are illustrated. It is shown that with the simultaneous left-right eigenvector assignment or the partial left-right eigenvector assignment techniques, both disturbance rejection and modal confinement or modal radiation reduction can be achieved, and thus the vibration amplitude in the concerned region or the sound pressure radiation at the receiver can be reduced significantly. Experimental efforts are performed to implement the new active control concepts for structural vibration control (Chapter 4), where the test results demonstrate the effectiveness of the proposed approaches.

Finally, in the last chapter of this thesis, the research efforts and achievements are summarized, and recommendations for possible future investigations are discussed.

TABLE OF CONTENTS

LIST OF FIGURES ix

LIST OF TABLES xii

NONMENCLATURE xiii

ACKNOWLEDGEMENTS xvii

Chapter 1 INTRODUCTION 1

1.1 Background 1
1.2 Literature Review 4
1.2.1 Right Eigenvector Assignment Approach 4
1.2.2 Left Eigenvector Assignment Approach 5
1.2.3 Simultaneous Left-Right Eigenvector Assignment Approach 6
1.2.4 Partial Left-Right Eigenvector Assignment Approach 7
1.2.5 Modal Tailoring Concept on Structural Acoustics Control 8
1.3 Problem Statements and Research Objectives 9
1.4 Thesis Outline 12

Chapter 2 STRUCTURAL VIBRATION CONTROL VIA SIMULTANEOUS LEFT-RIGHT EIGENVECTOR ASSIGNMENT 14

2.1 Introduction 14
2.2 Simultaneous Left-Right Eigenvector Assignment Method 15
2.3 Numerical Simulation on Forced Vibration Control Example 23
2.3.1 System Model 23
2.3.2 Case Studies and Analysis: Right Eigenvector Assignment Example 26
2.3.3 Case Studies and Analysis: Simultaneous Left-Right Eigenvector Assignment 30
2.3.4 Weighting Factor Selection for Left and Right Eigenvector Assignments 33
2.4 Summary 36

Chapter 3 STRUCTURAL VIBRATION CONTROL VIA PARTIAL LEFT-RIGHT EIGENVECTOR ASSIGNMENT 38

3.1 Introduction 38
3.2 Partial Left-Right Eigenvector Assignment Method and Algorithm 40
3.3 Numerical Simulations on Forced Vibration Control Example 46
3.3.1 Criteria of Selecting Left and Right Achievable Eigenvectors 46

3.3.2 Case Studies and Analysis: Partial Left-Right Eigenvector Assignment 48
3.4 Summary 57

Chapter 4 EXPERIMENTAL INVESTIGATION ON STRUCTUAL VIBRATION CONTROL TEST STAND 58

4.1 Introduction 58
4.2 Experimental Test Stand Hardware 59
4.3 System Identification 61
4.4 State Estimator 68
4.5 Controller Design 70
4.6 Modified Feedforward Configuration 74
4.7 Summary 77

Chapter 5 REDUCTION OF STRUCTURAL ACOUSTIC RADIATION VIA LEFT-RIGHT EIGENVECTOR ASSIGNMENT 78

5.1 Introduction 78
5.2 Modeling of Structural Acoustic Radiation 80
5.3 Left-Right Eigenvector Assignment Algorithm for Reduction of Structural Acoustic Radiation 83
5.3.1 Right Eigenvector Assignment: Modal Velocity Tailoring 83
5.3.2 Simultaneous Left-Right Eigenvector Assignment Algorithm 86
5.3.3 Partial Left-Right Eigenvector Assignment Algorithm 88
5.4 Numerical Simulations on Reduction of Structural Sound Pressure Radiation 89
5.4.1 Case Studies and Analysis: Simultaneous Left-Right Eigenvector Assignment 90
5.4.2 Case Studies and Analysis: Partial Left-Right Eigenvector Assignment 95
5.5 Summary 100

Chapter 6 CONCLUSIONS AND RECOMMENDATIONS 101

6.1 Summary of Research Effort and Achievements 101
6.2 Recommendations for Future Work 103
6.2.1 Simultaneous Suppression on Structural Vibration and Acoustic Radiation 104
6.2.2 Response Enhancement of Structural Vibration and Acoustic Radiation 104
6.2.3 Optimization of the Number and Location of Sensor/Actuator for Structural Vibration and Acoustic Control 105

Bibliography 106

Appendix A ANALYTICAL MODEL DERIVATION 111

A.1 Constitutive Equation of Piezoelectric Material 111
A.2 Integrated System of Beam Structure with Piezoelectric Actuator 112

LIST OF FIGURES

Figure 2-1: System arrangement consisting of host clamped-clamped beam, piezoelectric patches, and active control voltage inputs. External disturbance is exerted on point 7. 24

Figure 2-2: Frequency responses at point 1 w/ and w/o right eigenvector assignment method. 27

Figure 2-3: Modal energy distribution of all states w/ and w/o right eigenvector assignment method 29

Figure 2-4: Orthogonality indices w/ and w/o right eigenvector assignment method 29

Figure 2-5: Frequency responses at point 1 w/ and w/o simultaneous left-right eigenvector assignment method 31

Figure 2-6: Frequency responses at point 7 w/ and w/o simultaneous left-right eigenvector assignment method 31

Figure 2-7: Orthogonality indices w/ and w/o simultaneous left-right eigenvector assignment 32

Figure 2-8: Modal energy distribution of all states w/ and w/o simultaneous left-right eigenvector assignment 32

Figure 2-9: Left and right eigenvector error vs. weighting factor ratio 35

Figure 2-10: Performance prediction index vs. weighting factor ratio 36

Figure 3-1: Frequency responses at point 1 w/ and w/o partial left-right eigenvector assignment method 51

Figure 3-2: Orthogonality indices w/ and w/o partial left-right eigenvector assignment 52

Figure 3-3: Modal energy distribution of all states w/ and w/o partial left-right eigenvector assignment 53

Figure 3-4: Comparison of frequency responses at point 1 w/ pole placement, simultaneous left-right eigenvector assignment and partial left-right eigenvector assignment. 54

Figure 3-5: Comparison of frequency responses at point 7 w/ pole placement, simultaneous left-right eigenvector assignment and partial left-right eigenvector assignment. 55

Figure 4-1: Photograph of experimental setup. 59

Figure 4-2: Schematic of experimental setup 60

Figure 4-3: Mode shapes of first four modes with real modal coefficients 65

Figure 4-4: Frequency response function of velocity sensor to first input signal. 67

Figure 4-5: Frequency response function of velocity sensor to second input signal. 67

Figure 4-6: Frequency response function of velocity sensor to excitation signal. 68

Figure 4-7: Block diagram of the integrated system with state estimator 69

Figure 4-8: Performance prediction index vs. weighting factor ratio for the identified model. 72

Figure 4-9: Modified feedforward configuration. 75

Figure 4-10: Frequency response of velocity sensor to excitation signal w/ and w/o simultaneous left-right eigenvector assignment method 76

Figure 4-11: Frequency response of velocity sensor to excitation signal w/ and w/o partial left-right eigenvector assignment method 76

Figure 5-1: System arrangement consisting host clamped-clamped beam, piezoelectric patches, and active control voltage inputs. External disturbance is exerted on point 7. A microphone receiver is placed to detect the noise signal. 81

Figure 5-2: Left and right eigenvector error vs. weighting factor ratio 91

Figure 5-3: Performance prediction index vs. weighting factor ratio 91

Figure 5-4: Frequency response of sound pressure radiation at the microphone receiver with w_L/w_R=0.3104. 92

Figure 5-5: Frequency response of sound pressure radiation at the microphone receiver with w_L/w_R=0. 93

Figure 5-6: Modal radiation index analysis, w_L/w_R=0.3104 and w_L/w_R=0. 94

Figure **5-7**: Frequency response of sound pressure radiation at the microphone receiver (assigned left eigenvectors: 1st mode; assigned right eigenvectors: other modes). 97

Figure **5-8**: Orthogonality indices w/ and w/o partial left-right eigenvector assignment (assigned left eigenvectors: 1st mode)..... 98

Figure **5-9**: Modal radiation indices w/ and w/o partial left-right eigenvector assignment (assigned right eigenvectors: other mode except to 1st mode)..... 99

LIST OF TABLES

Table 2-1: Parameters of the system used in simulation.....24

Table 3-1: Total suppression in concerned coordinates at the first four resonant frequencies with different combinations of assigned left and right eigenvectors 50

Table 4-1: Results of experimental modal analysis 64

Table 5-1: Noise reduction at the microphone receiver at the first 9 resonant frequencies with different combinations of assigned left/right eigenvectors 96

NONMENCLATURE

A	State matrix in state space form
A_{beamj}	Finite element cross section area of beam structure
A_{PZTj}	Finite element cross section area of piezoelectric patch
B	Input matrix in state space form
B_0	Control input matrix
B_{eq}	Equivalent control input matrix
B_m	Modal input matrix
C	Output matrix in state space form
C_a	Sound speed in the medium
C_d	Damping matrix
D_j	Electrical displacement within the *j*-th piezoelectric patch
E	Disturbance distribution matrix in state space form
E_b	Young's Modulus of the beam structure
E_j	Electric field within the j-th piezoelectric patch
E_m	Modal energy level
E_p	Young's Modulus of the piezoelectric material
f	Excited force
F_d	Force distribution matrix
F_m	Modal force distribution matrix
h_{31}	Piezoelectric constant
I_{beam}	Moment of inertia of beam structure

I_{PZT}	Moment of inertia of piezoelectric patch
K	Feedback gain matrix
K_0	Stiffness matrix
K_1	Electromechanical coupling effect matrix of piezoelectric material
K_2	Inverse capacitance matrix of piezoelectric material
K_{eq}	Equivalent stiffness matrix
k	Wave number
M	Mass matrix
L	Output gain of state estimator
L_b	Length of beam structure
L_p	Length of piezoelectric patch
l_j	Finite element length
P	Radiated sound pressure
q	Displacement vector
Q	Electrical Charge vector
$\vec{R}$	Coordinate of microphone receiver
$\vec{r}_s$	Coordinate of surface
ΔS_j	Area of surface
T_{beam}	Kinetic energy of beam structure
T_{PZT}	Kinetic energy of piezoelectric patches
t_b	Thickness of beam structure
t_p	Thickness of piezoelectric patch

u	Control input in state space form
V	Control voltage
V_{beam}	Potential energy of beam structure
V_n	Surface velocity in normal direction
V_{PZT}	Potential energy of piezoelectric patches
w_b	Width of beam structure
w_e	Finite element transverse displacement and slope vector
w_L	Weighting factor for left eigenvector
w_p	Width of piezoelectric patch
w_R	Weighting factor for right eigenvector
X	x-coordinate of microphone receiver
x	State vector in state space form
Y	y-coordinate of microphone receiver
y	Output vector in state space form
β_{33}	Dielectric constant
$\mathrm{d}W$	Virtual work
¶	Material strain
$¶_L$	Left eigenvector error
$¶_R$	Right eigenvector error
z	Damping ratio
ρ_a	Density of air
ρ_b	Density of beam structure
ρ_p	Density of piezoelectric material

λ_j	Eigenvalue
Φ	Right eigenvector matrix
f_j	Right eigenvector
Y	Left eigenvector matrix
y_j	Left eigenvector
s_j	Orthogonality index
x	Performance prediction index
x_j	Modal radiation index
h	Modal coordinate vector
w_j	Natural frequency
t	Material stress

ACKNOWLEDGEMENTS

I would like to express the sincere appreciation to my thesis advisor, Professor Kon-Well Wang, for his excellent advice, guidance and support throughout my entire research. His knowledge and dedication have made my studying experience an invaluable step in my career. The appreciation is also extended to Dr. Chris Rahn, Dr. Mary Frecker and Dr. Heath Hofmann for serving on my Ph.D. committee and for their helpful advice and suggestions.

I am grateful to the National Science Foundation for providing financial support for this research.

Thanks to all fellow members of the Structural Dynamics and Controls Laboratory for the valuable discussions and suggestions during my stay in the SDCL. I would especially like to acknowledge Dr. Mike Philen for his guidance and assistance in the experimental works.

I am most grateful for the support and encouragement from my mother, my sisters, and all my family members. I would like to dedicate this Ph.D. thesis to my father, who always had provided me the best education environment and strongest encouragement all his life, and passed away in 1996.

Chapter 1

INTRODUCTION

1.1 Background

Structural vibration control and noise reduction is a common issue that engineers have to address in various industries. There are many mechanical components and systems, such as engine housing, fuselage panels, gearbox struts and machinery mounts, in which low vibration and noise transmission are desired to ensure human comfort, measurement accuracy, or expensive instrument protection.

Among the different control methods, the eigenstructure assignment approach has attracted considerable attention for active vibration suppression. The general eigenstructure assignment approach allocates not only the closed-loop eigenvalues if they are controllable, but also further shape the associated eigenvectors. It is well-known that the eigenvalues determine the system stability and dynamic characteristics. It is also known that the system eigenvectors are related to the system response distribution and disturbance rejection ability. Therefore, the eigenstructure assignment (assignment of eigenvalues and eigenvectors) method is an effective approach for active structure control

because the system dynamic behaviors are strongly governed by the eigenvalues and the corresponding eigenvectors.

The eigenstructure assignment method facilitates the control system through synthesizing a feedback gain matrix such that the closed-loop eigenvalues and eigenvectors can be placed according to the designer's wish. In general, the right eigenvectors of the system govern the response of each mode while the left eigenvectors are related to the system's response excited by the external excitations. The eigenstructure assignment approach can thus be divided into two portions, the right eigenvector assignment and left eigenvector assignment parts.

The right eigenvector assignment approach is directly related to the concept of mode shape tailoring, and thus has been utilized for vibration confinement applications. The principle of vibration confinement through right eigenvector assignment is to alter the closed-loop right eigenvectors such that the modal components corresponding to the concerned region have smaller amplitudes. As will be shown later in this thesis, the concept of right eigenvector assignment can be expanded to structural noise control as well, where one can alter the closed-loop right eigenvectors such that the modal velocity distribution of the mode shape will cause minimal sound radiation.

Most eigenstructure assignment approaches today have focused on right eigenvector shaping and vibration confinement. However, since such a technique only focuses on the tailoring of mode shapes, the absolute vibration amplitude of the concerned region of the structure might still be significant even though it is relatively low compared to other parts of the structure. Therefore, it is not guaranteed that the overall vibration response will always be suppressed.

Reciprocally with assigning right eigenvectors, the left eigenvector assignment method is related to the concept of changing the effects of the excitations on the system responses, and thus it can be utilized for disturbance rejection. There exist various analytical approaches to handle the disturbance rejection problems if the properties of external disturbances are known statistically, such as periodic disturbances (Bai and Wu, **1998**) or zeros mean white noise (Kwakernaak, **1972**). Robust control designs can also be applied to accommodate for exogenous disturbances and uncertainties but sacrificing the performance (Wei et al., **1992**; Konstanzer and Kroeplin, **1999**; Li et al., **2003**). In general, while most external disturbances in forced vibration problems are unknown, their space distributions are usually known. Therefore, the left eigenvector assignment method can be utilized for disturbance rejection in this type of forced vibration problems where the locations of excitation can be predicted. The principle of disturbance rejection through left eigenvector assignment is to alter the closed-loop left eigenvectors such that the left eigenvectors are as closely orthogonal to the disturbance distribution vectors (forcing vectors) as possible, and thus it can reduce the effects of external disturbances on the system responses.

For general non-self-adjoint systems, which are common with dissipated elements or active actions, the left and right eigenvectors are not the same and the system dynamics depends on both eigenvector sets. Therefore, to completely control the system responses, combining the two eigenvector assignment methods will provide us with the best design possibilities. In other words, the left-right eigenvector assignment approach can be used to concurrently achieve disturbance rejection, and modal confinement (vibration control purpose), or modal radiation reduction (noise control purpose).

Because of the clear physical meaning of the left and right eigenvectors, the left-right eigenvector assignment concept can target the nature of the structural vibration-acoustics problem with more physical insight as compared to many more classical control schemes.

1.2 Literature Review

1.2.1 Right Eigenvector Assignment Approach

Moore (**1976)** recognized the flexibility offered by state feedback in multi-input systems beyond the closed-loop eigenvalue assignment. In such a system, not only the closed-loop eigenvalues but also the eigenvectors can be assigned. This is now generally referred to the term "eigenstructure assignment". Some issues in linear control system were discussed by Andry et al. (**1983)** that the assignment of eigenstructure, in general, is possible only in multiple-inputs system, and the assigned eigenvectors must fall into admissible spaces. Kwon and Youn (**1987)** extended the previous theorem to the cases with repeated eigenvalues. Song and Jayasuriya (**1993**) utilized eigenvector assignment for mode localization in a multi-input-multi-output active vibration control system. In their method, the number of actuators requires the same as the number of the structural degrees of freedom. Choura (**1995)** and Choura and Yigit (**1995)** proposed to solve for the feedback gain matrices in vibration confinement problems by using an inverse eigenvalue problem method. In this method, a large number of actuators and sensors have to be used. Shelley and Clark (**2000b)** proposed a singular value decomposition

method to assign shaped right eigenvectors in a mode localization problem, and the feedback gain matrix is determined by the closest approximation to the desired right eigenvectors. Tang and Wang (**2004)** proposed a new vibration confinement technique through right eigenvector assignment in which the vibration energy can be confined in the unconcerned region of mechanical structure and the piezoelectric circuitry. The desired right eigenvectors are selected by minimizing the modal energy ratios of concerned modal energy relative to the total modal energy based on the Rayleigh Principle. Wu and Wang (**2004)** used the idea of combining a periodic structure and right eigenvector assignment to achieve vibration isolation design. This method can reduce the modal transmissibility from the exogenous excitation to the attenuated end of the isolator, and increase the stop band of the traditional passive isolator.

1.2.2 Left Eigenvector Assignment Approach

As discussed in **1.2.1**, the objective of most eigenstructure assignment methods applied to active vibration control is to alter the structural mode shapes. However, in forced vibration problems, the left eigenvectors also contribute to the vibration responses. The left eigenvectors are related to the effects of the external disturbance on the system responses, and thus required to be investigated concurrently. The concept of left eigenvector assignment is to modify the effects of the external excitations so that the system response can be changed.

Zhang et al. (**1990**) proposed a left eigenvector assignment method to suppress the vibration amplitude of a flexible beam. In this method, they considered the external

forces to be undesired inputs and achieved the disturbance rejection by altering the closed-loop left eigenvectors such that the closed-loop left eigenvectors are as closely orthogonal to the column vector of forcing matrix. Patton et al. (**1987)** demonstrated the left eigenvector assignment method on robust fault detection. In this approach, the assigning technique is the same as the right eigenvector assignment procedure in its dual controller design space. Burrows and Patton (**1992)** used a left eigenvector assignment approach for the observer design of a closed-loop system. The signal can be decoupled from the disturbances in this approach. Based on the bi-orthogonality condition between the right and left eigenvector matrices of the system, Choi et al. (**1995)** developed a flight control system in which both the disturbance suppressibility and controllability were considered by assigning the left eigenvectors.

1.2.3 Simultaneous Left-Right Eigenvector Assignment Approach

Due to the intrinsic characteristics of the system as aforementioned, in order to achieve disturbance rejection as well as modal confinement in a forced vibration problem, proper assignment of both the left and right eigenvectors is required.

Choi (**1998)** developed a simultaneous right and left eigenvector assignment method for a lateral flight control application. The bi-orthogonality condition between the left and right eigenvector matrices of the system as well as the relations between the achievable right modal matrix and states selection matrices are used to develop this methodology.

1.2.4 Partial Left-Right Eigenvector Assignment Approach

The achievable eigenvector set in the simultaneous left-right eigenvector assignment method proposed by Choi (**1998)** in **1.2.3** is determined based on the least square approximation. Since this method cannot exactly assign the eigenvectors, the least square error will always exist. Therefore the final system performance cannot be designed accurately. The simultaneous left-right eigenvector assignment approach tried to specify $2N$ eigenvectors (N left and N right eigenvectors). This is excessive since the protection methods (Davison and Wang, **1975;** Srinathkumar, **1978**) show that assigning N eigenvectors is sufficient to place N eigenvalues for an N-dimensional system. Therefore, this motivates the studies of partial left-right eigenvector assignment approach.

Fletcher (**1980**) presented an algorithm for an output feedback system through selecting left and right eigenvectors. This algorithm pointed out that the closed-loop eigenstructure assignable by output feedback is constrained by the requirement that the left and right eigenvectors must be in certain subspaces and the number of inputs plus the number of outputs exceeds the number of states. Fahmy and O'Reilly **(1988)** developed an efficient multistage parametric approach for eigenstructure assignment in linear multivariable output-feedback systems. This approach allows the subsets of left and right eigenvectors to be assigned in separate stages and thus the computational algorithm is relaxed from the orthogonality condition between the left and right eigenvectors. Roppenecker and O'Reilly (**1989)** presented the reduced orthogonality condition between the left and right eigenvectors by expressing the condition directly in terms of the

eigenvectors selected from the allowed subspaces. Clarke et al. (**2003)** presented a new method of output feedback eigenstructure assignment. A new reduced orthogonality condition between the left and right eigenvectors was derived so that the general formulation for the feedback gain matrix can be admitted, which utilized a two-stage design procedure.

1.2.5 Modal Tailoring Concept on Structural Acoustics Control

From the proposed investigation of structural vibration control in **1.1**, the structural response is directly governed by the system's right and left eigenvectors, which are related to the system's mode shapes and its ability of disturbance rejection, respectively. Since the structural noise radiation originates from the vibrating structure, one can also expand the concept of mode shape tailoring and disturbance rejection to address structural noise control by using different assigning strategies rather than vibration control methods.

It has been shown that significant suppressions in vibration levels do not necessarily imply significant reductions in radiated sound pressure levels (Baumann et al., **1991**; Baumann et al., **1992**; Dehandschutter et al., **1999**). Fuller and Burdisso (**1991**) also showed that sound attenuation in the far field can be achieved with a reduced control authority compared to the cases where all structural motion is cancelled.

The concept of structural modal shaping was introduced to account for the structural acoustics control problems in the past decade. Naghshineh and Koopmann (**1993**) presented the improved active structural acoustics control method based on the

minimization of the total power radiated from the vibrating structure expressed in terms of a truncated series sum. Each term of the sum is related to the coupling between the acoustic basis function of the radiation impedance matrix and the structural surface velocity vector. It has also been shown that the radiation modes can be calculated as the eigenvectors of an elemental radiation resistance matrix (Elliott and Johnson, **1993**). Constans et al. (**1998**) presented a numerical tool to minimize sound power from a vibrating shell structure. The optimal design of a weak radiator is achieved by tailoring the mode shapes through adding point masses, which is similar to the concept of right eigenvector assignment.

1.3 Problem Statements and Research Objectives

The literature review reveals that considerable amount research has been performed in structural vibration control through eigenstructure assignment techniques. However, the previous studies do not take both the left and right eigenvectors into consideration. In a general structural dynamics problem, the left and right eigenvectors are not the same and are related to different physical interpretations. In such a system, the right eigenvectors determine the individual modal responses while the left eigenvectors, reciprocally, determine the structural responses excited by external disturbances. Therefore it is reasonable to concurrently take both left and right eigenvectors into consideration in a structural vibration and noise control problem.

In the previous studies (Zhang et al., **1990;** Choi et al., **1995;** Choi, **1998**), one needs to pre-determine the desired closed-loop left eigenvectors *a priori* and enforce the elements of the desired left eigenvectors corresponding to nonzero elements of the forcing vector to be zeros. This will create two problems. First, the closed-loop left eigenvectors have to fall into certain admissible subspaces, hence the desired left eigenvectors may be highly different from the achievable eigenvectors. Second, theoretically, one only needs to minimize the inner product of each left eigenvector and each forcing vector, which means each left eigenvector is as closely orthogonal to each forcing vector as possible. Therefore, enforcing zeros into some elements of the desired left eigenvectors is not necessary. That may lead to unsatisfactory results while the controller tries to drive these elements to zeros rather than minimizes the inner products of the left eigenvectors and forcing vectors.

Furthermore, since structural acoustic radiation can be described by structural vibration behavior, the structural sound pressure radiation can be also decomposed into left and right eigenvectors. Although the concept of mode shape tailoring has been utilized in passive weak radiator design (Constans et al., **1998**), however, the disturbance rejection issue (left eigenvector concept) has not been addressed and the possible benefits of using active action has not been discussed. Therefore, it is reasonable to expand the concept of left-right eigenvector assignment for active control of structural noise radiation.

Based on the above discussions, the goal of this research is to investigate the feasibility of developing new left-right eigenvector assignment methods for active control of structural vibration and noise radiation. The literature review reveals that a few

investigations have been conducted in developing mathematical theories of left-right eigenstructure assignment for general control systems (Roppenecker and O'Reilly **1989;** Choi, **1998**; Clarke et al., **2003**). However, utilizing the left-right eigenvector assignment concept for structural vibration and acoustic controls has not been extensively explored.

In this research, the design criteria of eigenvectors are synthesized to satisfy the desired requirements in structural vibration and noise control applications, respectively. The closed-loop left eigenvectors will be altered so that the forcing vectors are as closely orthogonal to the left eigenvectors as possible. With this concept, the effects of external excitations on the system responses will be reduced. In this research, a new formulation is developed so that the desired closed-loop left eigenvectors are selected from certain admissible subspaces and decided through solving a generalized eigenvalue problem, where the orthogonality indices between the forcing vectors and the left eigenvectors are minimized. Reciprocally, to match the modal confinement requirement for vibration control purpose, the assigning strategy of right eigenvectors is to alter the closed-loop right eigenvectors such that the modal components corresponding to concerned region are as small as possible. Combining the Rayleigh Principle based right eigenvector assignment method (Tang and Wang, **2004**) and the minimized orthogonality index based left eigenvector assignment method, one can satisfy modal confinement and disturbance rejection concurrently for vibration control purpose. For structural noise control, the design criteria of left eigenvectors is the same as that in vibration control, that is to achieve disturbance rejection. Reciprocally, the right eigenvectors will be assigned such that the modal velocity distribution will cause minimal acoustic radiation. In this approach, the modal radiation indices will be minimized through solving a generalized

eigenvalue problem. Integrating the minimized orthogonality index and modal radiation index based left-right eigenvector assignment algorithm, one can achieve disturbance rejection and modal radiation reduction concurrently for structural noise control purpose. Conceptually, compared to many traditional control methods, the proposed eigenstructure assignment approach can provide more physical insight to the problem because both the left and right eigenvectors have clear physical meanings related to structural dynamics. Therefore, it may provide the best possibility to satisfy the structural vibration and noise control requirements.

1.4 Thesis Outline

This thesis consists of six chapters, which are organized as follows.

The first chapter introduces the background of this research. A review of the state of the art is presented. The problem statement and research objectives are stated.

The second chapter presents the structural vibration control approach by using the concepts of disturbance rejection and modal confinement through the simultaneous left-right eigenvector assignment approach. A fundamental understanding of the left and right eigenvector assignment method is provided. The design procedure and algorithm of this approach is stated. A clamped-clamped beam structure with piezoelectric actuators is used to illustrate the effectiveness of method.

The third chapter presents the study that investigates the feasibility of utilizing the partial left and right eigenvector assignment approach for structural vibration control.

The motivation of using this method and the algorithm and procedure are stated in this chapter. The same system example illustrated in Chapter 2 is used to evaluate the system performance.

The fourth chapter reports the experimental validation effort on structural vibration control through the left-right eigenvector assignment approaches. The test stand hardware and the system identification process are presented. A modified feedforward configuration is introduced to compensate for the system uncertainties and undesired noise so that the left-right eigenvector assignment algorithms can be implemented experimentally. The effectiveness of the proposed methods is illustrated.

The fifth chapter reports the study on expanding the left-right eigenvector assignment concept to achieve structural noise control. The mathematical expression of structural sound pressure radiation is formulated. The new tailoring strategy of mode shapes is derived. A clamped-clamped beam structure with piezoelectric actuators is utilized to illustrate the effectiveness of the left-right eigenvector assignment approaches for structural noise reduction.

Finally, the research efforts and achievements of this thesis are concluded and summarized in Chapter 6. The suggestions on possible future research directions and investigations are also provided.

Chapter 2

STRUCTURAL VIBRATION CONTROL VIA SIMULTANEOUS LEFT-RIGHT EIGENVECTOR ASSIGNMENT

2.1 Introduction

The purpose of the study discussed in the chapter is to investigate the feasibility of utilizing the simultaneous left and right eigenvector assignment method for active structural vibration control. The motivation is that while the right eigenvector assignment method can provide modal confinement as mentioned in Chapter 1, however, since such a technique only focuses on mode shape tailoring, the vibration level of the concerned region might still be significant even though it is relatively low compare to other parts of the structure. In other words, there is no guarantee that the overall vibration response will always be suppressed under external excitations. The concept of the right eigenvector assignment method for vibration confinement purpose is to alter the closed-loop system modes such that the modal components corresponding to the concerned region have relatively small amplitude. Reciprocally, the design goal of left eigenvector assignment is to alter the left eigenvectors of the closed-loop system so that they are as closely orthogonal to the system's forcing vectors as possible. For general non-self-adjoint systems (e.g., many systems with dissipative elements and/or feedback

actions), the right and left eigenvectors will not be the same and the system dynamics depends on both the eigenvector sets. Therefore, combining the two eigenvector assignment methods will provide us with the best design possibilities for a forced vibration control problem.

To advance the previous studies proposed by Zhang et al. (**1990**), Choi et al. (**1995)** and Choi (**1998)**, a new formulation of desired left eigenvectors is developed. In this new method, the desired left eigenvectors of the integrated system are selected from the admissible subspaces and decided through solving a generalized eigenvalue problem, where the orthogonality indices between the forcing vectors and the left eigenvectors are minimized. With this concept, the effects of external disturbance can be reduced. On the other hand, the components of right eigenvectors corresponding to the concerned regions are minimized concurrently.

The simultaneous left-right eigenvector assignment algorithm will be first discussed in the next section. Numerical simulations are then performed to evaluate the effectiveness of the proposed method in different case studies.

2.2 Simultaneous Left-Right Eigenvector Assignment Method

Consider a general linear time-invariant dynamical control system with full state feedback. The state equation can be described as

$$\begin{aligned} \dot{x} &= Ax + Bu + Ef \\ y &= Cx \\ u &= Kx \end{aligned} \tag{2.1}$$

where x is the $N\times1$ system state vector, A is the $N\times N$ state matrix, u is the $m\times1$ input vector, B is the $N\times m$ input matrix, f is the $l\times1$ external disturbance vector, E is the $N\times l$ disturbance distribution matrix, y is the $r\times1$ system output vector, C is the $r\times N$ output matrix, and K is the feedback gain matrix. The solution of the closed-loop state equation with zeros initial conditions can be described by the closed-loop eigenvalues and the corresponding right and left eigenvectors,

$$x(t) = \Phi\int_0^t e^{\Lambda(t-\tau)}\Psi^T Ef(\tau)d\tau = \sum_{k=1}^{l}\sum_{j=1}^{N}\phi_j(\psi_j^T e_k)\int_0^t e^{\lambda_j\tau}f(\tau)d\tau \tag{2.2}$$

where λ_j is the jth eigenvalue of the closed-loop system $(A+BK)$, f_j and ψ_j are its corresponding right and left eigenvectors, respectively, Λ is a diagonal matrix including all the closed-loop eigenvalues, and e_k is the kth column vector of disturbance distribution matrix E.

This equation shows that the state response of the closed-loop system $x(t)$ depends on the right eigenvectors which determine the response of each mode, and the left eigenvectors which determine the response excited by external disturbances. The goal of the simultaneous left-right eigenvector assignment is to determine a feedback gain matrix K such that the left and right eigenvectors are assigned concurrently for disturbance rejection and modal confinement, respectively.

The closed-loop system can be expressed by its eigenvalues and corresponding left and right eigenvectors in the state space form, i.e.

$$\begin{aligned}(A+BK-\lambda_j I_N)\phi_j &= 0\\ (A^T+K^TB^T-\lambda_j I_N)\psi_j &= 0\end{aligned} \quad j=1,2,...,N \tag{2.3}$$

In this investigation, we assume that all eigenvalues of the closed-loop system are different from the open-loop ones. If the closed-loop eigenvalue is complex, its complex conjugate eigenvalue will exist simultaneously. Equation **2.3** can be re-written as

$$\begin{aligned}\left[A-\lambda_j I_N \mid B\right]\begin{Bmatrix}\phi_j\\ K\phi_j\end{Bmatrix} &= 0\\ \left[A^T-\lambda_j I_N \mid I_N\right]\begin{Bmatrix}\psi_j\\ K^TB^T\psi_j\end{Bmatrix} &= 0\end{aligned} \quad j=1,2,...,N \tag{2.4}$$

We define

$$\begin{aligned}T_j &= \left[A-\lambda_j I_N \mid B\right]\\ P_j &= \left[A^T-\lambda_j I_N \mid I_N\right]\end{aligned} \quad j=1,2,...,N \tag{2.5}$$

and then take singular value decomposition of T_j and P_j. Equation **2.5** can be described as

$$\begin{aligned} T_j &= \left[A - \lambda_j I_N \mid B \right] = U_j^{(R)} \left[D_j \mid 0 \right] V_j^{(R)*} \\ P_j &= \left[A^T - \lambda_j I_N \mid I_N \right] = U_j^{(L)} \left[D_j \mid 0 \right] V_j^{((L)*} \end{aligned} \quad j = 1, 2, ..., N \tag{2.6}$$

where $U_j^{(\cdot)}$ and $V_j^{(\cdot)}$ are the left and right singular vector matrices (Klema and Laub, **1980**) which satisfy the unitary condition, i.e.,

$$\begin{aligned} U_j^{(\cdot)*} U_j^{(\cdot)} &= I \\ V_j^{(\cdot)*} V_j^{(\cdot)} &= I \end{aligned} \quad j = 1, 2, ..., N \tag{2.7}$$

Since we assume all closed-loop eigenvalues are different from the open-loop ones, $A - \lambda_j I_N$ and $A^T - \lambda_j I_N$ are nonsingular and D_j will be a positive definite diagonal matrix containing all the singular values of T_j and P_j. The matrix $V_j^{(\cdot)}$ can be partitioned as

$$V_j^{(\cdot)} = \begin{bmatrix} v_{j1}^{(\cdot)} & v_{j2}^{(\cdot)} \\ v_{j3}^{(\cdot)} & v_{j4}^{(\cdot)} \end{bmatrix}, \quad j = 1, 2, ..., N \tag{2.8}$$

where $v_{j2}^{(R)}$, $v_{j4}^{(R)}$, $v_{j2}^{(L)}$, and $v_{j4}^{(L)}$ are $N \times m$, $m \times m$, $N \times N$, and $N \times N$ submatrices. Hence it is easy to verify the following equations.

$$T_j \begin{bmatrix} v_{j2}^{(R)} \\ v_{j4}^{(R)} \end{bmatrix} = U_j^{(R)} \begin{bmatrix} D_j \mid 0 \end{bmatrix} V_j^{(R)*} \begin{bmatrix} v_{j2}^{(R)} \\ v_{j4}^{(R)} \end{bmatrix} = U_j^{(R)} \begin{bmatrix} D_j \mid 0 \end{bmatrix} \begin{bmatrix} 0 \\ I \end{bmatrix} = 0$$
$$P_j \begin{bmatrix} v_{j2}^{(L)} \\ v_{j4}^{(L)} \end{bmatrix} = U_j^{(L)} \begin{bmatrix} D_j \mid 0 \end{bmatrix} V_j^{(L)*} \begin{bmatrix} v_{j2}^{(L)} \\ v_{j4}^{(L)} \end{bmatrix} = U_j^{(L)} \begin{bmatrix} D_j \mid 0 \end{bmatrix} \begin{bmatrix} 0 \\ I \end{bmatrix} = 0 \qquad (2.9)$$

Equation **2.9** means that the matrix $\begin{bmatrix} v_{j2}^{(\bullet)} \\ v_{j4}^{(\bullet)} \end{bmatrix}$ spans the null space of T_j and P_j. By comparing Equation **2.4** and Equation **2.9**, one can conclude that the admissible closed-loop left and right eigenvectors must be the linear combinations of the column vectors of $v_{j2}^{(\bullet)}$ (Cunningham, **1980**; Corr and Clark, **1995**; Shelley and Clark, **2000b**), i.e.

$$\begin{aligned} \phi_j &= v_{j2}^{(R)} \mu_j \\ \psi_j &= v_{j2}^{(L)} \gamma_j \end{aligned} \quad j = 1, 2, \ldots, N \qquad (2.10)$$

where μ_j and γ_j are $m \times 1$ and $N \times 1$ scalar vectors.

As the design criteria for disturbance rejection expressed above, the closed-loop left eigenvectors should be assigned so that each closed-loop left eigenvector is as closely orthogonal to the forcing vector e_k as possible. Here we first define the orthogonality index σ_j as

$$\sigma_j = \frac{\sum_{k=1}^{l} (\psi_j^* e_k)^2}{\left|\psi_j\right|^2 \sum_{k=1}^{l} \left|e_k\right|^2} \qquad (2.11)$$

The left eigenvector assignment approach in this research is to choose the scalar vector γ_j appropriately so that the orthogonality index σ_j is minimized. Therefore, one can formulate this idea as following,

$$\min \frac{\psi_j^{d*}(\sum_{k=1}^{l} e_k e_k^T)\psi_j^d}{(\sum_{k=1}^{l} e_k^T e_k)\psi_j^{d*}\psi_j^d} = \min \frac{\gamma_j^* v_{j2}^{(L)*}(\sum_{k=1}^{l} e_k e_k^T)v_{j2}^{(L)}\gamma_j}{\gamma_j^*(\sum_{k=1}^{l} e_k^T e_k)v_{j2}^{(L)*}v_{j2}^{(L)}\gamma_j}, \quad j = 1,2,...,N \qquad (2.12)$$

We define

$$\begin{aligned} X_j &= v_{j2}^{(L)*}(\sum_{k=1}^{l} e_k e_k^T)v_{j2}^{(L)} \\ Y_j &= (\sum_{k=1}^{l} e_k^T e_k)v_{j2}^{(L)*}v_{j2}^{(L)} \end{aligned} \qquad (2.13)$$

Hence Equation **2.12** can be re-written as

$$\min \frac{\gamma_j^* v_{j2}^{(L)*}(\sum_{k=1}^{l} e_k e_k^T)v_{j2}^{(L)}\gamma_j}{\gamma_j^*(\sum_{k=1}^{l} e_k^T e_k)v_{j2}^{(L)*}v_{j2}^{(L)}\gamma_j} = \min \frac{\gamma_j^* X_j \gamma_j}{\gamma_j^* Y_j \gamma_j} = \left|\beta_j\right|_{\min}, \quad j = 1,2,...,N \qquad (2.14)$$

Equation **2.14** is equivalent to solve for the following generalized eigenvalue problem,

$$X_j \gamma_j = \beta_{jk} Y_j \gamma_j, \quad j,k = 1,2,...,N \tag{2.15}$$

where β_{jk} is the eigenvalue of Equation **2.15**. The minimal ratio $|\beta_j|_{\min}$ in Equation **2.15** is the minimal eigenvalue among β_{jk} and γ_j is its corresponding eigenvector. Once the scalar vector γ_j is determined, we can form the desired left eigenvector matrix by substituting γ_j into Equation **2.10**,

$$\Psi^d = \left[v_{12}^{(L)} \gamma_1, v_{22}^{(L)} \gamma_2, ..., v_{N2}^{(L)} \gamma_N \right] = \left[\psi_1^d, \psi_2^d, ..., \psi_N^d \right] \tag{2.16}$$

Consider the orthogonality condition between the right and left eigenvector matrices,

$$\Psi^T \Phi = I \tag{2.17}$$

and the problem is thus formulated to minimize the following performance index

$$J_{1j} = \left\| (\Psi^d)^T \phi_j - I_j \right\|^2, \quad j = 1,2,...,N \tag{2.18}$$

where I_j is the jth column of identity matrix I. On the other hand, we also want to minimize the modal components of the right eigenvectors corresponding to the concerned regions for vibration confinement purpose, and hence we can formulate this concept by minimizing the following performance index

$$J_{2j} = \left\| b\phi_j \right\|^2, \quad j = 1, 2, ..., N \tag{2.19}$$

where b is Boolean matrix to extract the components of the right eigenvectors corresponding to the concerned regions.

Combining the idea presented above, Equation **2.10**, Equation **2.18** and Equation **2.19**, the overall simultaneous left-right eigenvector assignment approach can be formulated such that the following performance index is minimized (Choi, **1998**),

$$J_j = \min_{\mu_j} \left\| \begin{bmatrix} w_L (\Psi^d)^T v_{j2}^{(R)} \\ w_R b v_{j2}^{(R)} \end{bmatrix} \{\mu_j\} - \begin{Bmatrix} w_L I_j \\ 0 \end{Bmatrix} \right\|^2, \quad j = 1, 2, ..., N \tag{2.20}$$

where w_L and w_R are the weighting factors on the left and right eigenvectors respectively. The optimal solution of Equation **2.20** can be determined by letting $dJ_j/d\mu_j=0$, that

$$\tilde{\mu}_j = \left(\begin{bmatrix} w_L (\Psi^d)^T v_{j2}^{(R)} \\ w_R b v_{j2}^{(R)} \end{bmatrix}^* \begin{bmatrix} w_L (\Psi^d)^T v_{j2}^{(R)} \\ w_R b v_{j2}^{(R)} \end{bmatrix} \right)^{-1} \begin{bmatrix} w_L (\Psi^d)^T v_{j2}^{(R)} \\ w_R b v_{j2}^{(R)} \end{bmatrix}^* \begin{Bmatrix} w_L I_j \\ 0 \end{Bmatrix}, \tag{2.21}$$
$$j = 1, 2, ..., N$$

Substitute $\tilde{\mu}_j$ into Equation **2.10** and Equation **2.4**, we can obtain the following

$$\begin{aligned} \phi_j^a &= v_{j2}^{(R)} \tilde{\mu}_j, \quad \Phi^a = \left[\phi_1^a, \phi_2^a, ..., \phi_N^a \right] \\ w_j &= K\phi_j^a = v_{j4}^{(R)} \tilde{\mu}_j, \quad W = \left[w_1, w_2, ..., w_N \right] \end{aligned} \tag{2.22}$$

where f_j^a is the *j*th achievable right eigenvector. If the matrix $[\Phi^a B]$ is full rank (Clarke et al., **2003**), then there exists a real feedback gain matrix *K* that is solved as (Andry et al., **1983**; Kwon and Youn, **1987**)

$$K = W(\Phi^a)^{-1} \tag{2.23}$$

2.3 Numerical Simulation on Forced Vibration Control Example

In this section, we will illustrate the control results of the forced vibration problem and examine the theoretical predictions by numerical simulation.

2.3.1 System Model

As shown in Figure **2-1**, the host clamped-clamped beam structure is assumed to be made of aluminum. Four sets of piezoelectric patches are bonded onto the top surface of the beam. Each of the piezoelectric patches connects to a voltage source as the active control input. An external force is exerted on point 7. The integrated system is

discretized and modeled by finite element method (FEM). All the system parameters are listed in Table **2-1**.

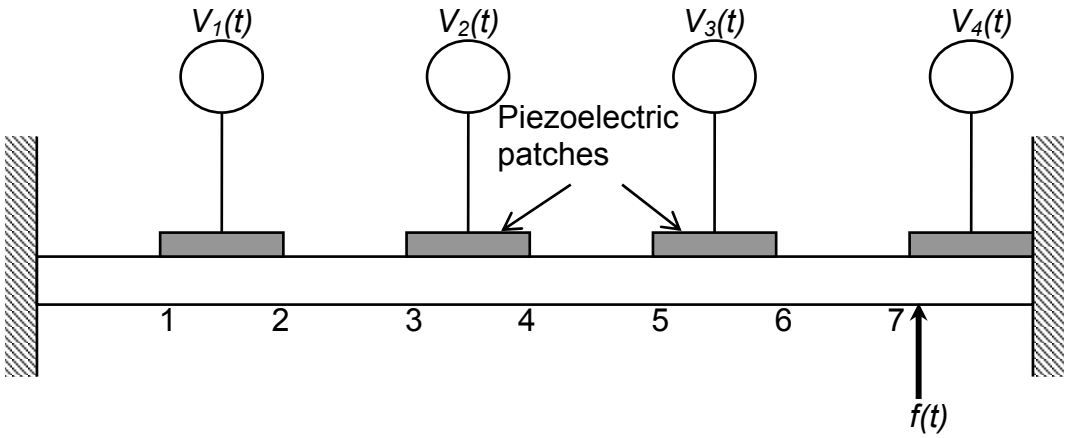

Figure **2-1**: System arrangement consisting of host clamped-clamped beam, piezoelectric patches, and active control voltage inputs. External disturbance is exerted on point 7.

Table **2-1**: Parameters of the system used in simulation

E_b=3.1×10^{10} *Pa*	E_p=7.40×10^{10} *Pa*
ρ_b=2700 *Kg/m*^{3}	ρ_p=7600 *Kg/m*^{3}
ζ=0.008	t_p=2.5×10^{-4} *m*
L_b=0.2524 *m*	w_b=0.020 *m*
L_p=0.03155 *m*	w_p=0.020 *m*
t_b=0.0030 *m*	h_{31}=7.664×10^8 *N/C*
β_{33}=7.3310×10^7 *V*	

The discretized equations of motion for the integrated system can be described as

$$\begin{aligned} M\ddot{q} + C_d\dot{q} + K_0 q + K_1 Q &= F_d f \\ K_1^T q + K_2 Q &= B_0 V \end{aligned} \tag{2.24}$$

where M, C_d and K_0 are the $2n \times 2n$ mass, damping and stiffness matrices of the structure, q is the $2n \times 1$ structural transverse displacement and slope vector, Q is the $m \times 1$ electric charge vector, K_2 is the $m \times m$ inverse capacitance matrix of the piezoelectric patches, K_1 is the $2n \times m$ matrix which represents the electromechanical coupling effect of the piezoelectric materials, F_d is the external force distribution vector, B_0 is the $m \times m$ control input matrix and V is the $m \times 1$ active control input vector. Equation **2.24** can be merged as

$$M\ddot{q} + C_d\dot{q} + (K_0 - K_1 K_2^{-1} K_1^T)q = F_d f - K_1 K_2^{-1} B_0 V \tag{2.25}$$

and then transformed to the state-space form as Equation **2.1**,

$$\begin{aligned} x &= \begin{Bmatrix} q \\ \dot{q} \end{Bmatrix}, \quad A = \begin{bmatrix} 0 & I_n \\ -M^{-1}K_{eq} & -M^{-1}C_d \end{bmatrix}, \quad B = \begin{bmatrix} 0 \\ M^{-1}B_{eq} \end{bmatrix}, \\ E &= \begin{bmatrix} 0 \\ M^{-1}F_d \end{bmatrix}, \quad u = V \end{aligned} \tag{2.26}$$

where $K_{eq}=K_0-K_1K_2^{-1}K_1^T$ and $B_{eq}=-K_1K_2^{-1}B_0$.

2.3.2 Case Studies and Analysis: Right Eigenvector Assignment Example

As mentioned earlier, we summarize that the vibration amplitude of the concerned region may not always be reduced by modal confinement technique through right eigenvector assignment method in a forced vibration problem. Since such a technique only focuses on the tailoring of mode shapes, the structural vibration level of the concerned region might still be significant even though it is relatively low compare to other part of the structure. It is also noted from Equation **2.2** that the vibration response $x(t)$ depends on not only the right eigenvectors (mode shape concept), but also the product of left eigenvectors and disturbance distribution (disturbance rejection concept). In this section we will illustrate an example to show this hypothesis.

As shown in Figure **2-1**, the integrated beam structure is utilized for demonstration. The vibration suppression is needed in the concerned region, point 1 through point 4 of the beam. The desired closed-loop eigenvalues have to be decided *a priori*. In this example, we choose the desired closed-loop eigenvalues to be 5.000 times the real part and 1.006 times the imaginary part of the open-loop ones so that we do not change the resonant frequencies significantly but increase the damping of the closed-loop system.

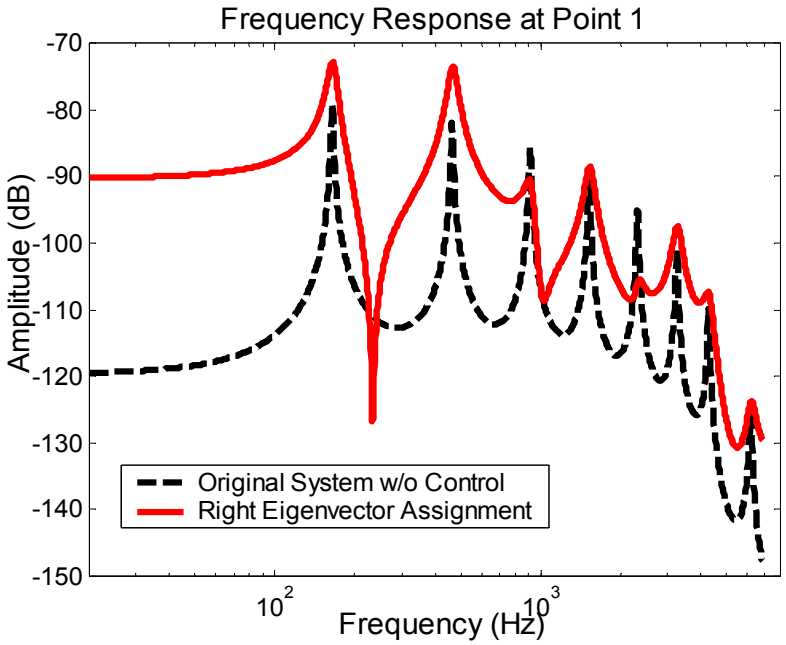

Figure **2-2**: Frequency responses at point 1 w/ and w/o right eigenvector assignment method.

Figure **2-2** shows the frequency response of the displacement relative to the external force at point 1 of the beam. The vibration amplitude of this point (also in other points of concerned region) increases after the right eigenvector assignment method is applied. In order to analyze the mode shape distribution, the modal energy level E_m can be defined as

$$E_m = \sum_{j=1}^{N} \left\{ t_{j1}^2, t_{j2}^2, \ldots, t_{jN}^2 \right\}^T \qquad (2.27)$$

where t_{ji} is the component of the jth right eigenvector. Figure **2-3** shows the modal energy distribution of all states corresponding to the displacements and the velocities.

The states 1 through 13 are related to structural displacements, and the states 15 through 27 related to structural velocities corresponding to points 1 through 7 of the beam. Figure **2-4** shows the orthogonality indices of the selected modes. A smaller index σ_j means the left eigenvector is more closely orthogonal to the forcing vector and hence better disturbance rejection. Even though the modal energy, both potential energy (related to displacements) and kinetic energy (related to velocities) is reduced in states 1 through 9 and states 15 through 25 by this method as shown in Figure **2-3**, the orthogonality indices of several modes are still higher than the original system after the active control is applied as shown in Figure **2-4**. This example shows the arguments as aforementioned that the vibration amplitude in the concerned region of the beam cannot always be suppressed by pure right eigenvector assignment method. Therefore it is intuitive to utilize the simultaneous left-right eigenvector assignment approach for forced vibration problems.

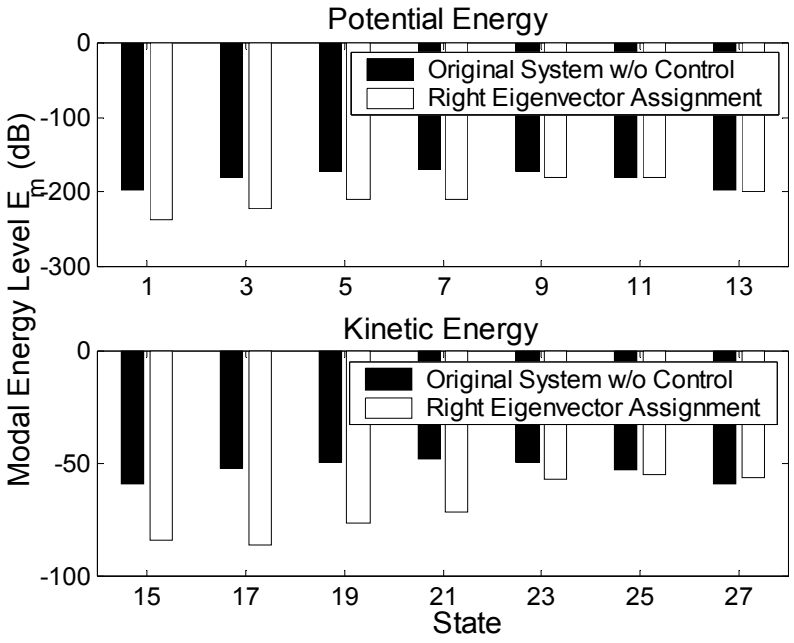

Figure 2-3: Modal energy distribution of all states w/ and w/o right eigenvector assignment method

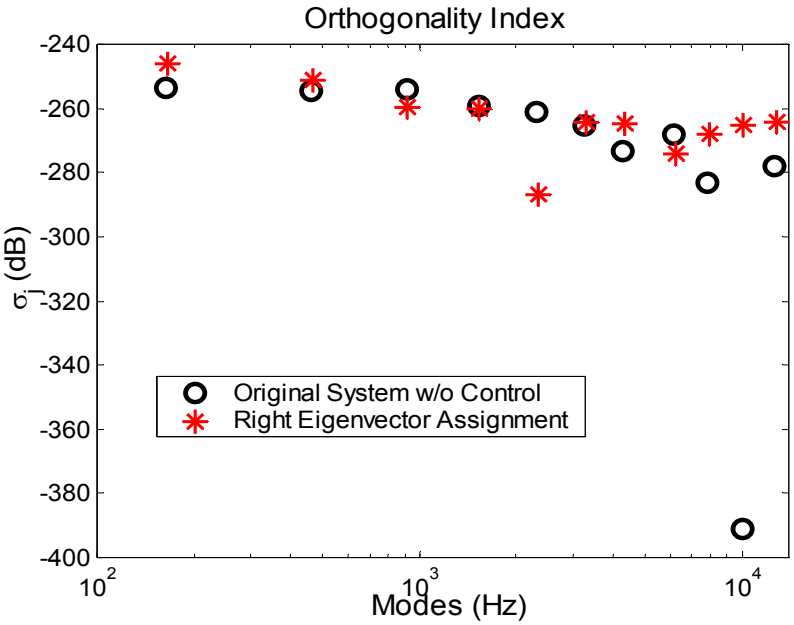

Figure 2-4: Orthogonality indices w/ and w/o right eigenvector assignment method

2.3.3 Case Studies and Analysis: Simultaneous Left-Right Eigenvector Assignment

Figure **2-5** and Figure **2-6** show the frequency responses of the displacement relative to the external force at point 1 and point 7 with w_L=4.040 (weighting factor for left eigenvector assignment) and w_R=1 (weighting factor for right eigenvector assignment). The same set of closed-loop eigenvalues as in **2.3.2** is used in this case. Figure **2-5** shows that the vibration amplitude at point 1 (also in other points of the concerned region) has been suppressed significantly throughout the broad frequency range by the simultaneous left-right eigenvector assignment method. It is also noted that compared with the original system without active control, the vibration amplitude at point 7 becomes larger at the resonant frequencies higher than 1K Hz as shown in Figure **2-6**. The phenomenon is reasonable since modal energy has been confined in the unconcerned region as a result of the right eigenvector assignment contribution.

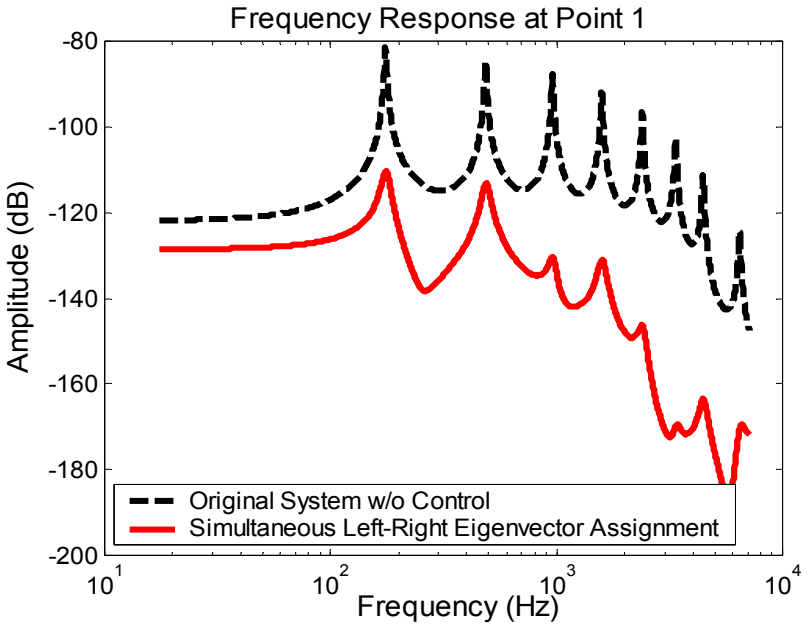

Figure 2-5: Frequency responses at point 1 w/ and w/o simultaneous left-right eigenvector assignment method

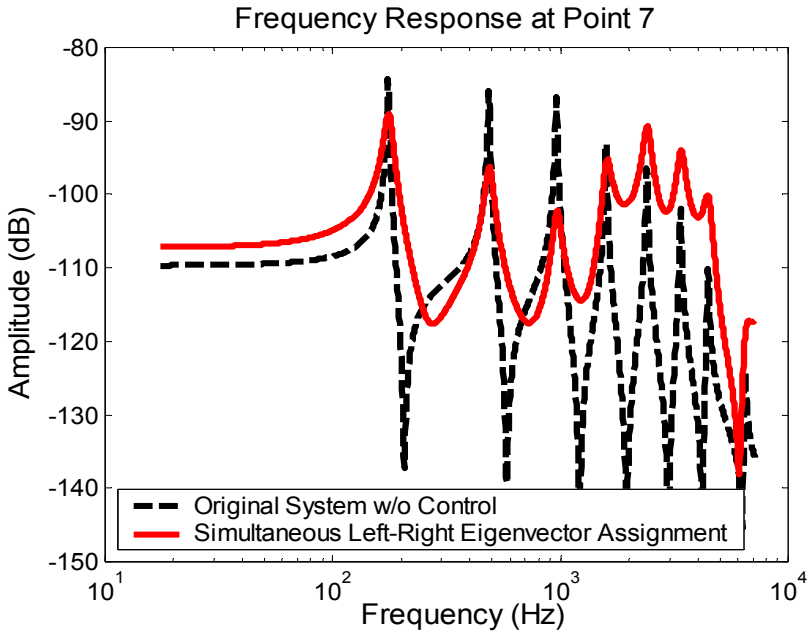

Figure 2-6: Frequency responses at point 7 w/ and w/o simultaneous left-right eigenvector assignment method

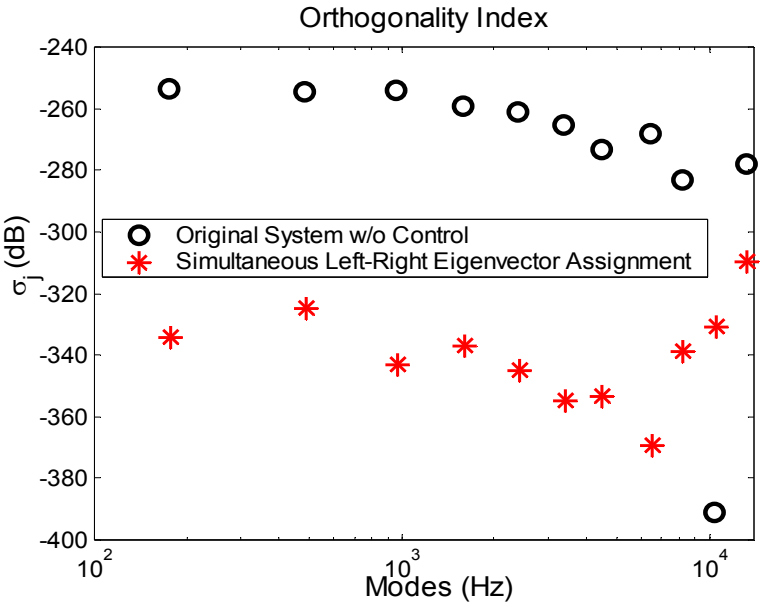

Figure 2-7: Orthogonality indices w/ and w/o simultaneous left-right eigenvector assignment

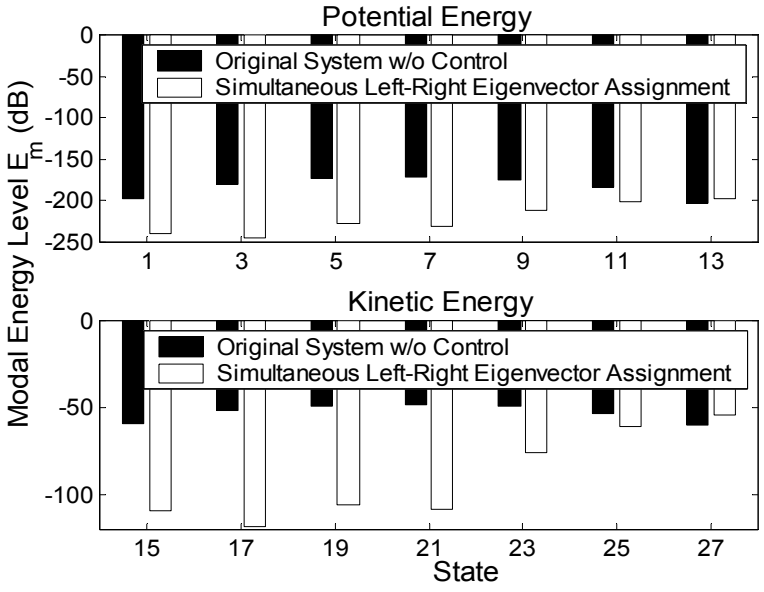

Figure 2-8: Modal energy distribution of all states w/ and w/o simultaneous left-right eigenvector assignment

Figure **2-7** shows the orthogonality indices of the selected modes. It shows that with the simultaneous left-right eigenvector assignment approach, the orthogonality indices are reduced except to the 10^{th} mode at 10.481 KHz. Figure **2-8** shows the modal energy distribution of all the states corresponding to the displacements (states 1 through 13 related to points 1 through 7) and the velocities (states 15 through 27). It shows that the modal energy has been re-distributed after the active control is applied. Both the potential energy (related to the displacements) and kinetic energy (related to the velocities) decrease significantly in states 1 through 11 and states 15 through 25. On the other hand, the modal energy levels increase in the other states (states 13 and 27) of the unconcerned region, indicating that some modal energy has been confined in this region. Conclusively, the analysis results have demonstrated that the simultaneous left-right eigenvector assignment approach can successfully achieve disturbance rejection (as shown in Figure **2-7** and modal confinement (as shown in Figure **2-8**) concurrently.

2.3.4 Weighting Factor Selection for Left and Right Eigenvector Assignments

The solution in Equation **2.21** is determined based on the least square approximation. Therefore, the desired left and right eigenvectors can not be assigned exactly. On the other hand, the solutions and control performance may be sensitive to the weighting factors in the formulation. Due to these reasons, this study is to investigate the effect of the weighting factors. In this section, we will discuss the relationship of the right eigenvector error versus the weighting factor ratio (left weighting factor/right

weighting factor), the left eigenvector error versus the weighting factor ratio, and the performance prediction index versus the weighting factor ratio.

From Equation **2.19**, the right eigenvector error is define to be

$$\varepsilon_R = \sum_{j=1}^{N} \varepsilon_{R_j} = \sum_{j=1}^{N} \left| \frac{\phi_j^{a*} b^T b \phi_j^a}{\phi_j^{a*} \phi_j^a} \right| \tag{2.28}$$

where f_j^a is the jth achievable right eigenvector. On the other hand, the left eigenvector error is defined as

$$\varepsilon_L = \sum_{j=1}^{N} \varepsilon_{L_j} = \sum_{j=1}^{N} \left\| \frac{\psi_j^d}{\|\psi_j^d\|} - \frac{\psi_j^a}{\|\psi_j^a\|} \right\|_2 \tag{2.29}$$

where ψ_j^d is the jth desired left eigenvector as in Equation **2.16** and ψ_j^a is the jth achievable left eigenvector of Ψ^a ($=[(\Phi^a)^{-1}]^T$) that is obtained through the orthogonality condition between the left and right eigenvector matrices. Figure **2-9** shows the right and left eigenvector errors versus weighting factor ratio w_L/w_R. The overall trend of the two curves indicates that the right eigenvector errors become larger with increasing weighting factor ratios, while the left eigenvector errors are reduced with increasing weighting factor ratios. In order to find a weighting factor ratio such that the most suppression effects can be achieved, one can define the performance prediction index to be the product of the right and left eigenvector errors, i.e.

$$\xi = \sum_{j=1}^{N} \varepsilon_{R_j} \varepsilon_{L_j} \tag{2.30}$$

Figure **2-10** shows the performance prediction index versus weighting factor ratio. The minimal performance prediction index in this example is obtained at w_L/w_R=4.040. The control performance of this case with w_L/w_R=4.040 through the simultaneous left-right eigenvector assignment method are shown as in Figure **2-5** and Figure **2-6**.

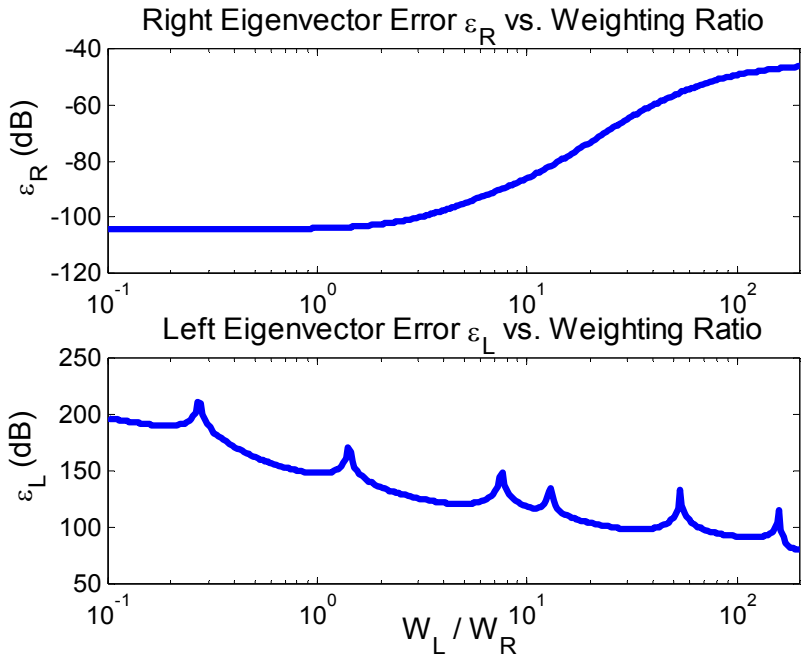

Figure **2-9**: Left and right eigenvector error vs. weighting factor ratio

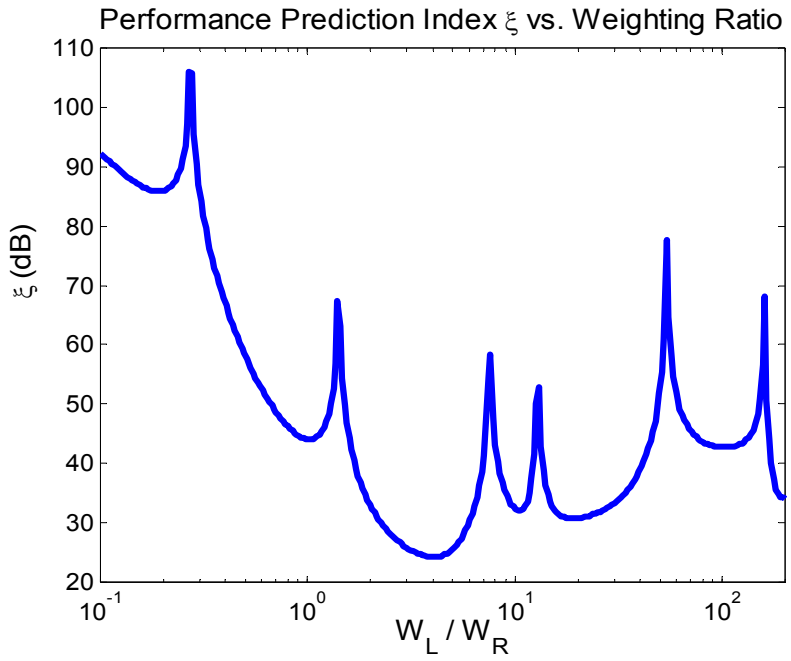

Figure **2-10**: Performance prediction index vs. weighting factor ratio

2.4 Summary

A simultaneous left-right eigenvector assignment for both disturbance rejection and modal confinement in a structural vibration control problem is investigated and reported in this chapter. A new formulation to select the desired closed-loop left eigenvectors by minimizing the orthogonality indices is derived. A method to choose the weighting factors is also provided. The effectiveness of the proposed method is demonstrated through numerical simulations on a clamped-clamped beam structure example. Conclusively, this approach can successfully achieve both disturbance rejection

and modal confinement concurrently, and thus can enhance the vibration suppression performance in the concerned region of the beam structure.

Chapter 3

STRUCTURAL VIBRATION CONTROL VIA PARTIAL LEFT-RIGHT EIGENVECTOR ASSIGNMENT

3.1 Introduction

The purpose of the research presented in this chapter is to investigate the feasibility of utilizing the partial left and right eigenvector assignment method for active structural vibration control.

In Chapter 2, it is shown that the solution of the simultaneous left-right eigenvector assignment method is determined through a generalized inverse, based on least square approximation. While the method is promising, it is generally difficult to predict the least square error and determine the system performance. Furthermore, the solution of the least square approximation and hence control performance can be sensitive to the weighting factors in the formulation. Since it is difficult to quantify the contributions of the left and right eigenvectors at certain resonant frequencies individually, there is no rigorous rule to decide the weighting factors for general cases. It is thus necessary to utilize significant computational efforts in deciding the weighting factors as discussed in **2.3.4**.

Clarke et al. (**2003**) proposed an algorithm in which the reduced number of selected left and right eigenvectors can be exactly assigned as the desired ones for an output feedback system without approximation. The motivation of the research presented in this chapter is to utilize this control theory and derive the corresponding design strategy for structural vibration control. In such an algorithm, both the selected left and right eigenvectors can be exactly assigned so that the disturbance rejection as well as modal confinement can be achieved concurrently.

To satisfy disturbance rejection, the selected desired left eigenvectors are determined by minimizing the orthogonality indices so that they are as closely orthogonal to the forcing vectors as possible. On the other hand, to achieve modal confinement, the remaining desired right eigenvectors are determined by minimizing the ratio of concerned area modal energy relative to the total modal energy based on the Rayleigh Principle so that the modal components corresponding to the concerned coordinates are as small as possible (Tang and Wang, **2004**). Therefore, the two criteria of assigning the selected left and right eigenvectors can be used for a forced vibration control problem.

In the next section, the partial left-right eigenvector assignment algorithm will be discussed. Numerical simulations are then performed to evaluate the effectiveness of the proposed method on the clamped-clamped beam structure.

3.2 Partial Left-Right Eigenvector Assignment Method and Algorithm

To discuss the partial left-right eigenvector assignment method, we first consider a general linear time-invariant dynamical control system with output feedback,

$$\begin{aligned} \dot{x} &= Ax + Bu + Ef \\ y &= Cx \\ u &= Ky \end{aligned} \tag{3.1}$$

where x is the $N\times1$ system state vector, A is the $N\times N$ state matrix, u is the $m\times1$ input vector, B is the $N\times m$ input matrix, f is the $l\times1$ external disturbance vector, E is the $N\times l$ disturbance distribution matrix, y is the $r\times1$ system output vector, C is the $r\times N$ output matrix, and K is the feedback gain matrix. The objective of this method is to determine a feedback gain matrix K such that the total N closed-loop left and right eigenvectors are exactly assigned as the desired ones in which the disturbance rejection and modal confinement can be achieved simultaneously.

The closed-loop system can be expressed by its eigenvalues and the corresponding right and left eigenvectors in the state space form similarly as in Equation **2.3**,

$$\begin{aligned} &(A + BKC - \lambda_j I_N)\phi_j = 0 \\ &(A^T + C^T K^T B^T - \lambda_j I_N)\psi_j = 0 \end{aligned} \quad j = 1, 2, ..., N \tag{3.2}$$

In this investigation, we also assume that all eigenvalues of the closed-loop system are different from the open-loop ones as discussed in Chapter 2. Equation **3.2** can be re-written as

$$\begin{aligned} &\left[A-\lambda_j I_N \mid B\right]\begin{Bmatrix}\phi_j \\ KC\phi_j\end{Bmatrix}=0 \\ &\left[A^T-\lambda_j I_N \mid C^T\right]\begin{Bmatrix}\psi_j \\ K^T B^T\psi_j\end{Bmatrix}=0 \end{aligned} \quad j=1,2,...,N \qquad (3.3)$$

With the same procedure as in Chapter 2, we define

$$\begin{aligned} T_j &= \left[A-\lambda_j I_N \mid B\right] \\ P_j &= \left[A^T-\lambda_j I_N \mid C^T\right] \end{aligned} \quad j=1,2,...,N \qquad (3.4)$$

and then take singular value decomposition of T_j and P_j. The admissible right and left eigenvectors can be obtained by spanning the admissible subspaces v_{j2} and m_{j2} (Choi, **1998**; Shelley and Clark, **2000b**; Tang and Wang, **2004**; Wu and Wang, **2004**) respectively, i.e.

$$\begin{aligned} \phi_j &= v_{j2}\mu_j \\ \psi_j &= m_{j2}\gamma_j \end{aligned} \quad j=1,2,...,N \qquad (3.5)$$

where μ_j and γ_j are $m\times1$ and $r\times1$ scalar vector. The left and right eigenvectors have to satisfy the orthogonality condition, i.e.

$$\psi_i^T \phi_j = 0 \quad for \quad all \quad i \neq j \tag{3.6}$$

The orthogonality condition in Equation **3.6** requires *2N* eigenvectors to be assigned, however, only *N* closed-loop eigenvalues are allocated. The protection methods (Davison and Wang, **1975**; Srinathkumar, **1978**) show that assigning *N* eigenvectors is sufficient to place *N* eigenvalues. Therefore the following theorem will depict this condition (Clarke et al., **2003**).

Theorem: The eigenvalue λ_j is assignable if there exists ψ_j and f_j spanned by the admissible subspace as described in Equation **3.5**, such that

(a) rank($C[\mathsf{f}_1, \mathsf{f}_2,.., \mathsf{f}_p]$)=$p$ and $\lambda_j = \bar{\lambda}_k$ implies $\phi_j = \bar{\phi}_k$

(b) rank($B^T[\psi_{p+1}, \psi_{p+2},.., \psi_N]$)=$N$-$p$ and $\lambda_j = \bar{\lambda}_k$ implies $\psi_j = \bar{\psi}_k$

(c) $\psi_i^T \phi_j = 0$ for all $j=1,2,...,p;\ i=p+1,\ p+2,..N$

The proof of this theorem can be seen in Clarke et al. (**2003**).

We assume *p* closed-loop right eigenvectors are first derived from the admissible subspaces as in Equation **3.5**,

$$\Phi_p^a = \left[\phi_1^a, \phi_2^a, ..., \phi_p^a\right] = \left[v_{12}\mu_1, v_{22}\mu_2, ...v_{p2}\mu_p\right]$$
$$W_p = KC\Phi_p^a = \left[w_1, w_2, ..., w_p\right] = \left[v_{14}\mu_1, v_{24}\mu_2, ...v_{p4}\mu_p\right] \quad (3.7)$$

and then impose the "achievable" right eigenvectors on the second part of Equation **3.3** to satisfy the orthogonality condition, constraint (c) of the theorem, i.e.

$$\begin{bmatrix} A^T - \lambda_j I_N & C^T \\ (\Phi_p^a)^T & 0 \end{bmatrix} \begin{Bmatrix} \psi_j \\ K^T B^T \psi_j \end{Bmatrix} = 0, j = p+1, p+2, ..., N \quad (3.8)$$

As the same steps as stated earlier, we define

$$P_j' = \begin{bmatrix} A^T - \lambda_j I_N & C^T \\ (\Phi_p^a)^T & 0 \end{bmatrix} \quad (3.9)$$

and then take singular value decomposition of P_j'. Therefore we can obtain the null space of P_j' and then determine the achievable left eigenvectors by spanning the "achievable" subspaces of the left eigenvectors, i.e.

$$\Psi_p^a = \left[\psi_{p+1}^a, \psi_{p+2}^a, ..., \psi_N^a\right] = \left[m'_{p+1,2}\gamma_{p+1}, m'_{p+2,2}\gamma_{p+2}, ..., m'_{N2}\gamma_N\right]$$
$$Z_p = K^T B^T \Psi_p^a = \left[z_{p+1}, z_{p+2}, ..., z_N\right] = \left[m'_{p+1,4}\gamma_{p+1}, m'_{p+2,4}\gamma_{p+2}, ..., m'_{N4}\gamma_N\right] \quad (3.10)$$

where m'_{j2} is a Nä(r-p) matrix for the "achievable" subspace of left eigenvector and γ_j is a (r-p)ä1 scalar vector.

Alternatively, we assume N-p closed-loop left eigenvectors are first derived from the admissible subspaces as in Equation **3.5**,

$$\begin{aligned} \Psi_p^a &= \left[\psi_{p+1}^a, \psi_{p+2}^a, ..., \psi_N^a\right] = \left[m_{p+1,2}\gamma_{p+1}, m_{p+2,2}\gamma_{p+2}, ..., m_{N2}\gamma_N\right] \\ Z_p &= K^T B^T \Psi_p^a = \left[z_{p+1}, z_{p+2}, ..., z_N\right] = \left[m_{p+1,4}\gamma_{p+1}, m_{p+2,4}\gamma_{p+2}, ..., m_{N4}\gamma_N\right] \end{aligned} \quad (3.11)$$

and then impose the "achievable" left eigenvectors on the first part of Equation **3.3** to satisfy the orthogonality condition, i.e.

$$\begin{bmatrix} A - \lambda_j I_N & B \\ (\Psi_p^a)^T & 0 \end{bmatrix} \begin{Bmatrix} \phi_j \\ KC\phi_j \end{Bmatrix} = 0 \quad (3.12)$$

Similarly as the previous steps, we define

$$T'_j = \begin{bmatrix} A - \lambda_j I & B \\ (\Psi_p^a)^T & 0 \end{bmatrix} \quad (3.13)$$

After determining the null space of T'_j, we can obtain the "achievable" subspaces for the right eigenvectors and then determine the achievable right eigenvectors, i.e.

$$\Phi_p^a = \left[\phi_1^a, \phi_2^a, ..., \phi_p^a\right] = \left[v'_{12}\mu_1, v'_{22}\mu_2, ...v'_{p2}\mu_p\right]$$
$$W_p = KC\Phi_p^a = \left[w_1, w_2, ..., w_p\right] = \left[v'_{14}\mu_1, v'_{24}\mu_2, ...v'_{p4}\mu_p\right] \quad (3.14)$$

where v'_{j2} is a $N\times(m+p-N)$ matrix for the "achievable" subspace of right eigenvector and μ_j is a $(m+p-N)\times 1$ scalar vector. If Φ_p^a and Ψ_p^a satisfy the constraint (a) and (b) of the theorem, the feedback gain matrix is thus obtain (Clarke et al., **2003**) as

$$K = ((\Psi_p^a)^T B)^\dagger Z_p^T + W_p(C\Phi_p^a)^\dagger - ((\Psi_p^a)^T B)^\dagger Z_p^T C\Phi_p^a (C\Phi_p^a)^\dagger \quad (3.15)$$

where $(\bullet)^\dagger$ denotes the generalized inverse of (∏).

It is noted that when either the right or left eigenvectors are first determined in the procedure, m (input number), r (output number), and p (assigned right eigenvector number) have to satisfy the constraints. The rank constraints (a) and (b) of the theorem dictate that the number of assignable right eigenvector can not be more than r and the number of assignable left eigenvector can not be more than m. Equation **3.8** and Equation **3.12** also show that the assigned right eigenvector number, p, and the assigned left eigenvector number, $(N-p)$, have to satisfy these constraints if the null spaces of T_j' and P_j' are not empty. While the left eigenvectors are first assigned, the extra constraint is that the number of assignable left eigenvector $(N-P)$ is less than m. Conversely if the right eigenvectors are first determined, an extra constraint, $p<r$, has to be imposed. It is also noted that the eigenvectors that are first determined have larger achievable spaces for

assigning. Therefore the eigenvectors that are dominant in performance should be first assigned.

3.3 Numerical Simulations on Forced Vibration Control Example

In this section, we will use the same clamped-clamped beam structure system in Figure **2-1** as an example to illustrate the control results and examine the theoretical predictions through numerical simulation. All the system parameters are listed in Table **2-1**.

3.3.1 Criteria of Selecting Left and Right Achievable Eigenvectors

The design criteria of the left eigenvectors for disturbance rejection purpose is to assign specific closed-loop left eigenvectors so that the desired closed-loop left eigenvectors are as closely orthogonal to the forcing vectors e_k as possible. Based on this concept, the desired left eigenvector is determined by minimizing the orthogonality indices as the design steps expressed in Chapter 2,

$$\min \frac{\psi_j^{d*}(\sum_{k=1}^{l} e_k e_k^T)\psi_j^d}{(\sum_{k=1}^{l} e_k^T e_k)\psi_j^{d*}\psi_j^d} = \min \frac{\gamma_j^* m_{j2}^* (\sum_{k=1}^{l} e_k e_k^T) m_{j2}\gamma_j}{\gamma_j^* (\sum_{k=1}^{l} e_k^T e_k) m_{j2}^* m_{j2}\gamma_j} = \left|\beta_j\right|_{\min}, \quad (3.16)$$

$$j = p+1, p+2, ..., N$$

The scalar vector g_j for synthesizing the desired left eigenvectors can be determined through solving a generalized eigenvalue problem,

$$X_j \gamma_j = \beta_{jk} Y_j \gamma_j \qquad (3.17)$$

where $X_j = m_{j2}^* (\sum_{k=1}^{l} e_k e_k^T) m_{j2}$, and $Y_j = (\sum_{k=1}^{l} e_k^T e_k) m_{j2}^* m_{j2}$. The minimal ratio $|\beta_j|_{\min}$ in Equation **3.16** is the minimal eigenvalue among b_{jk} and γ_j is its corresponding eigenvector.

Reciprocally, the design criteria of the right eigenvectors for modal confinement is to assign the remaining closed-loop right eigenvectors so that the desired closed-loop right eigenvectors have as small components corresponding to the concerned region as possible. This concept can be realized by minimizing the modal energy ratio of the concerned region modal energy relative to the total modal energy

$$\min \frac{\phi_j^* b^T S b \phi_j}{\phi_j^* S \phi_j} = \min \frac{\mu_j^* v_{j2}^* b^T S b v_{j2} \mu_j}{\mu_j^* v_{j2}^* S v_{j2} \mu_j} = |\alpha_j|_{\min}, \quad j = 1, 2, ..., p \qquad (3.18)$$

where $S = \begin{bmatrix} K_{eq} & 0 \\ 0 & M \end{bmatrix}$, and b is the Boolean matrix representing the concerned coordinates and the remaining coordinates of the closed-loop right eigenvector.

Based on the Rayleigh Principle (Meirovitch, **1980**), the scalar vector μ_j for synthesizing the desired right eigenvectors can be determined through solving the generalized eigenvalue problem (Tang and Wang, **2004**),

$$\Lambda_j \mu_j = \alpha_{jk} \Omega_j \mu_j \qquad (3.19)$$

where $\Lambda_j = v_{j2}^* b^T S b v_{j2}$, and $\Omega_j = v_{j2}^* S v_{j2}$. The minimal modal energy ratio $|\alpha_j|_{\min}$ is the minimal eigenvalues among α_{jk} and μ_j is its corresponding eigenvector.

3.3.2 Case Studies and Analysis: Partial Left-Right Eigenvector Assignment

In this test bed example, since the control input number *m*, is 4 and all eigenvalues are complex, two left eigenvectors (a complex conjugate pair) are selected to be first assigned in the partial left-right eigenvector assignment algorithm. This is because the number of assigned left eigenvectors has to be less than the input number and the complex conjugate pair of the eigenvectors has to exist simultaneously. We choose the output number to be (*N-2*) so that all numbers, *m*, *r* and *p*, satisfy the constraints. The remaining (*N-2*) right eigenvectors are assigned in the second step after the two left eigenvectors are first assigned. Since the complex conjugate pairs of eigenvectors have to exist simultaneously, we cannot arbitrarily assign both the left and right eigenvectors corresponding to the same complex conjugate pair of eigenvalues concurrently. Conceptually, the left and right eigenvectors cannot be assigned focusing on the same

resonant frequencies simultaneously. It is also noted that it is difficult to evaluate the contributions of the left and right eigenvectors separately for the control performance at different resonant frequencies. However, the combination number of the total N assigned left and right eigenvectors corresponding to the different eigenvalues is very limited. Therefore the optimal solution can be obtained by selecting the case of most suppression among all the achievable combinations without paying heavy computational efforts.

The criteria for selecting the best combination of assigned left and right eigenvectors is to select the case in which the most suppression effect is achieved in all the concerned coordinates at the resonant frequencies. In this simulation example, the same set of desired closed-loop eigenvalues as in Chapter 2 is used. Table **3-1** lists the total frequency response suppressions of structural vibration at point 1 through point 4 (concerned coordinates) focusing on the first four resonant frequencies with different combinations of assigned left and right eigenvectors. The top row indicates the first four resonant peaks and the left column indicates the eigenvalues corresponding to the two left eigenvectors which will be first assigned. The middle arrays indicate the total vibration suppression on point 1 through point 4 at each resonant frequency with each assigned combination respectively. The smaller magnitude in the middle arrays means more vibration suppression. It is determined that the most suppression performance, as shown in the summation column, can be obtained in the shaded case of Table **3-1**.

Table 3-1: Total suppression in concerned coordinates at the first four resonant frequencies with different combinations of assigned left and right eigenvectors

Suppression (dB) / Eigenvalue	1st Resonant Peak 176.1655 Hz	2nd Resonant Peak 488.1796 Hz	3rd Resonant Peak 964.7710 Hz	4th Resonant Peak 1595.6997 Hz	Summation
-121.9505 ≤ 3067.3225i	-75.4241	-165.8650	-78.5494	-23.7370	-343.5755
-241.0339 ≤ 6061.8366i	4.1400	-16.9012	-99.4555	14.3826	-97.8341
-398.6438 ≤ 10026.0760i	-10.4917	-34.7706	-19.2776	-71.2914	-135.8313
-846.6194 ≤ 21291.7977i	6.0983	13.9728	12.3894	-8.1486	24.3119
-1118.7197 ≤ 28134.8746i	-81.7825	-55.6646	-54.7616	-65.8452	-258.0539
-1619.8745 ≤ 40738.2656i	-18.1940	-35.3669	-54.0730	-19.1778	-126.8117
-2056.1936 ≤ 51712.0089i	21.6258	6.2653	-85.4116	-47.6497	-105.1702
-3312.7089 ≤ 83311.7658i	21.8795	30.9404	42.8908	52.7116	148.4223
-4258.3065 ≤ 107093.0265i	-123.6421	-99.7633	-114.7339	-97.6091	-435.7484
-6119.7848 ≤ 153906.0730i	51.8113	54.2799	54.4475	108.3536	268.8923

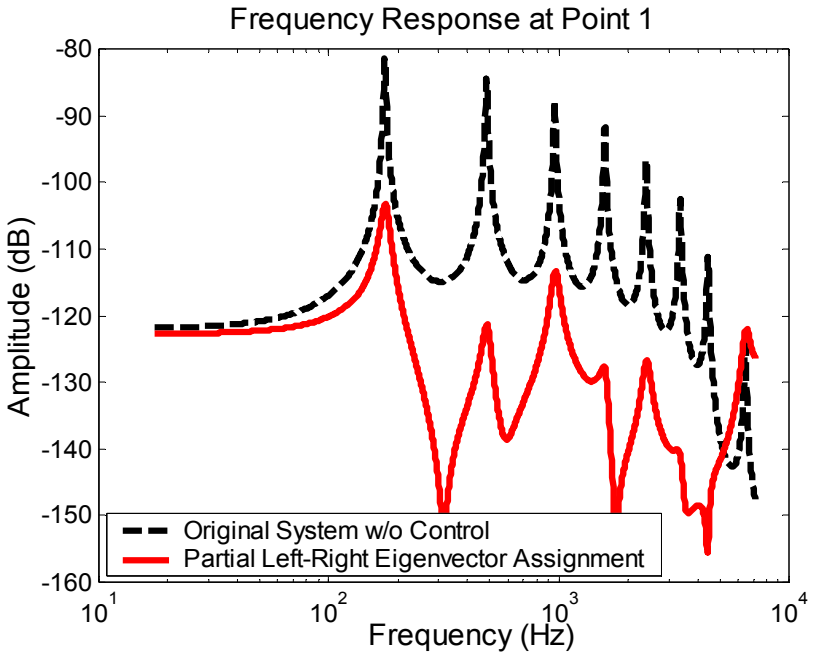

Figure **3-1**: Frequency responses at point 1 w/ and w/o partial left-right eigenvector assignment method

Figure **3-1** shows the frequency response of the displacement relative to the external force at point 1 by the optimal combination of assigned left and right eigenvectors. In this case, the left eigenvectors corresponding to the 12th mode (the eigenvalues are -4258.307≤107093.027i) are first assigned and then the right eigenvectors corresponding to the remaining modes are assigned in the second step. Figure **3-1** shows that through partial left-right eigenvector assignment, the vibration amplitude can be suppressed significantly at point 1 (also at other points of the concerned region) throughout the broad frequency range including the first 7 resonant frequencies.

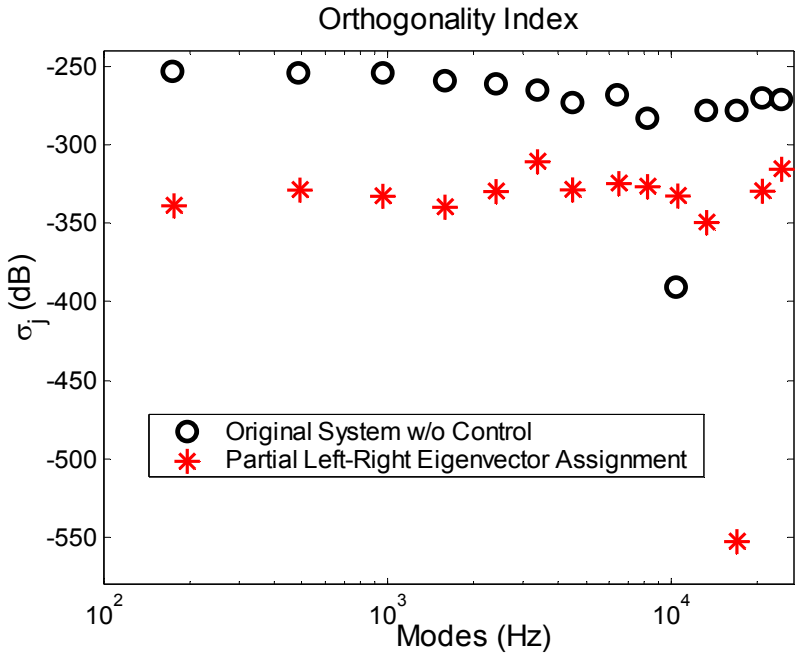

Figure **3-2**: Orthogonality indices w/ and w/o partial left-right eigenvector assignment

Figure **3-2** shows the orthogonality indices of the selected system modes. It is shown that all the orthogonality indices can be reduced by the partial left-right eigenvector assignment approach except the 10^{th} mode at 10.481 KHz. In other words, the system capability of disturbance rejection can be improved by this approach. It is also noted that with this method the orthogonality index at the 12^{th} mode (17044.384 Hz) is reduced significantly because the left eigenvectors corresponding to this mode are assigned exactly.

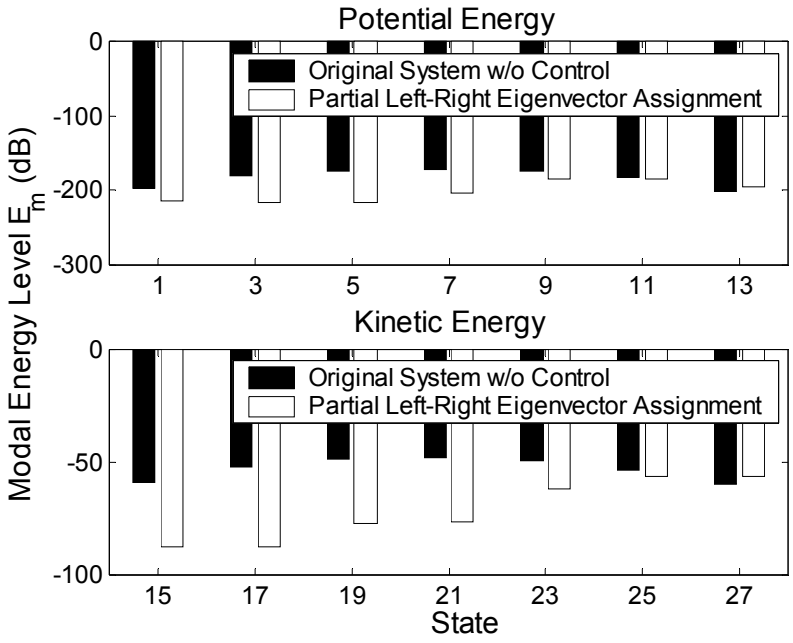

Figure **3-3**: Modal energy distribution of all states w/ and w/o partial left-right eigenvector assignment

Figure **3-3** shows the modal energy distribution of all the system states corresponding to the displacements (states 1 through 13 related to point 1 through 7) and the velocities (states 15 through 27). With this method, all the right eigenvectors except the 12^{th} mode are exactly assigned by minimizing the modal energy ratios. It shows that the modal energy has been re-distributed after the active control is applied. Both the potential modal energy (related to the displacements) and kinetic modal energy (related to the velocities) decrease in states 1 through 11 and states 15 through 25. On the other hand, the modal energy levels increase in the other states (state 13 and state 27) of the unconcerned region, indicating that some modal energy has been confined in this region. Compared with Figure **2-3** which shows the modal energy distribution with right

eigenvector assignment, the concerned modal energy using the partial left-right eigenvector assignment method is larger (particularly in potential energy) than that with the pure right eigenvector assignment. The reason is that the right eigenvectors (except the two corresponding to the 12^{th} mode) are assigned after first assigning the left eigenvectors in this approach, therefore the achievable subspaces for right eigenvectors become smaller due to the orthogonality condition imposed. Conclusively, the analysis results have demonstrated that the partial left-right eigenvector assignment approach can successfully achieve disturbance rejection (as shown in Figure **3-2**) and modal confinement (as shown in Figure **3-3**).

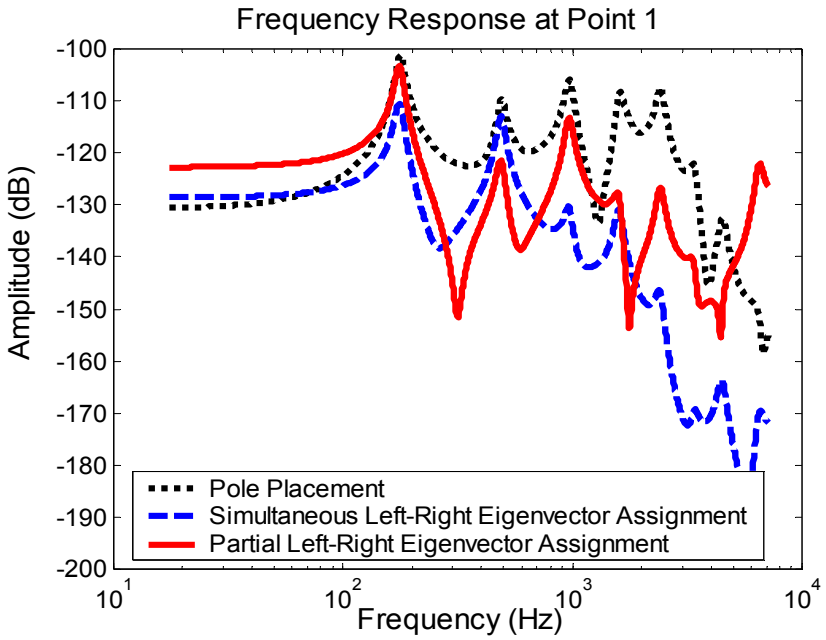

Figure **3-4**: Comparison of frequency responses at point 1 w/ pole placement, simultaneous left-right eigenvector assignment and partial left-right eigenvector assignment.

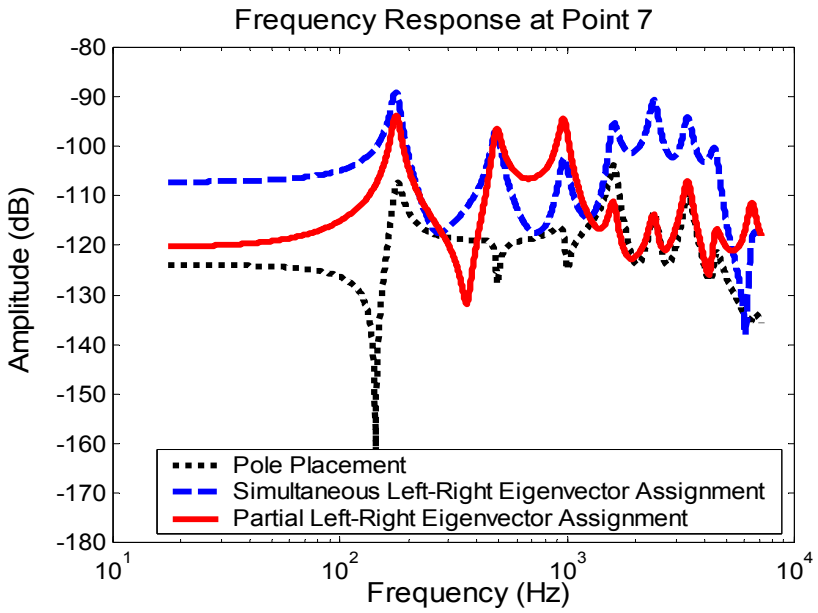

Figure 3-5: Comparison of frequency responses at point 7 w/ pole placement, simultaneous left-right eigenvector assignment and partial left-right eigenvector assignment.

Figure **3-4** and Figure **3-5** show the comparison of frequency responses of the displacement at point 1 and point 7 through the pole placement method, simultaneous left-right eigenvector assignment method and partial left-right eigenvector assignment method respectively with the same set of desired eigenvalues. It is noted that both the simultaneous left-right eigenvector assignment and partial left-right eigenvector assignment methods can achieve more vibration suppression at point 1 (also at the other points of concerned region) than the pole placement method throughout the broad frequency range. On the other hand, the vibration amplitude becomes larger at point 7 (the unconcerned region) with both the simultaneous left-right eigenvector assignment and partial left-right eigenvector assignment methods than with the pole placement

method. Conceptually the pole placement method does not focus on the performance in the specific coordinates and does not consider the external disturbances. However, both the simultaneous left-right eigenvector assignment and partial left-right eigenvector assignment methods use the same set of closed-loop eigenvalues, and then focus on the concerned coordinates. The disturbance rejection is also considered in these two methods. Therefore both the simultaneous left-right eigenvector assignment and partial left-right eigenvector assignment methods can be utilized to further enhance the suppression performance in the concerned region from the baseline of the pole placement method with the same desired closed-loop eigenvalue set.

It is also noted that the vibration suppression performance at some resonant frequencies is worse using the partial left-right eigenvector assignment method than using the simultaneous left-right eigenvector assignment method. Even though in this example, the suppression performance at certain resonant peaks is better with simultaneous left-right eigenvector assignment than that with partial left-right eigenvector assignment, the computation efficiency of the two algorithms must be indicated and addressed. The solution of simultaneous left-right eigenvector assignment approach is determined based on the least square approximation and it is normally difficult to predict the least square error and the control performance. Furthermore, the solution and performance may be very sensitive to the weighting factors. Since there is no rigorous rule to choose the optimal weighting factors in general cases so that the most suppression effects can be achieved, it is necessary to pay heavy computational efforts to decide the optimal weighting factors. However, the partial left-right eigenvector assignment approach can exactly assign all the selected desired left and right eigenvectors without approximation.

The optimal case of the partial left-right eigenvector assignment method can be easily obtained among the limited combination number of different assigned left and right eigenvectors cases without heavy computational efforts. In general, the control performance with different methods is case-dependent. One should not conclude that the simultaneous left-right eigenvector assignment approach always outperforms the partial left-right eigenvector assignment method or vice versa. The partial left-right eigenvector assignment method is an alternative method to achieve satisfactory system performance with more efficient computation effort, as compared to the simultaneous left-right eigenvector assignment approach.

3.4 Summary

A partial left-right eigenvector assignment for both disturbance rejection and modal confinement is explored for structural vibration control. The selected left and right eigenvectors can be assigned exactly without approximation. The desired left eigenvectors are determined by minimizing the orthogonality indices so that the disturbance rejection can be achieved. The desired right eigenvectors are selected by minimizing the modal energy ratios. Through numerical simulations, the effectiveness of the proposed method is demonstrated on a clamped-clamped beam structure example. Conclusively, this method can successfully achieve both disturbance rejection and modal confinement concurrently, and thus its vibration confinement/suppression performance can be enhanced as compared to the baseline system with the same eigenvalues via pole-placement.

Chapter 4

EXPERIMENTAL INVESTIGATION ON STRUCTUAL VIBRATION CONTROL TEST STAND

4.1 Introduction

The objective of the research presented in this chapter is to implement the left-right eigenvector assignment algorithms experimentally, and validate the effectiveness of the proposed approach for structural vibration control. The test stand is a clamped-clamped beam structure, with piezoelectric strips bonded on the surface of the beam as actuators and exciter. The experimental setup, including the beam structure, measurement instruments, actuation devices, and PC-based data acquisition system will be introduced in the next section. A system identification procedure, utilizing the modal analysis technique and structured state-space parameterization, is performed to identify the system model. A modified feedforward configuration is introduced to accommodate for the system uncertainties and undesired noise. Both the simultaneous and partial left-right eigenvector assignment methods are implemented to evaluate their vibration control performance.

4.2 Experimental Test Stand Hardware

Figure **4-1** shows the photograph of the experimental setup, which consists of a clamped-clamped beam structure, signal analyzer and function generator, laser vibrometer sensing instrument, smoothing low pass filter, power amplifier and dSPACE data acquisition system. Figure **4-2** shows the schematic of the experimental setup and the dimension of the integrated piezoelectric-beam structure.

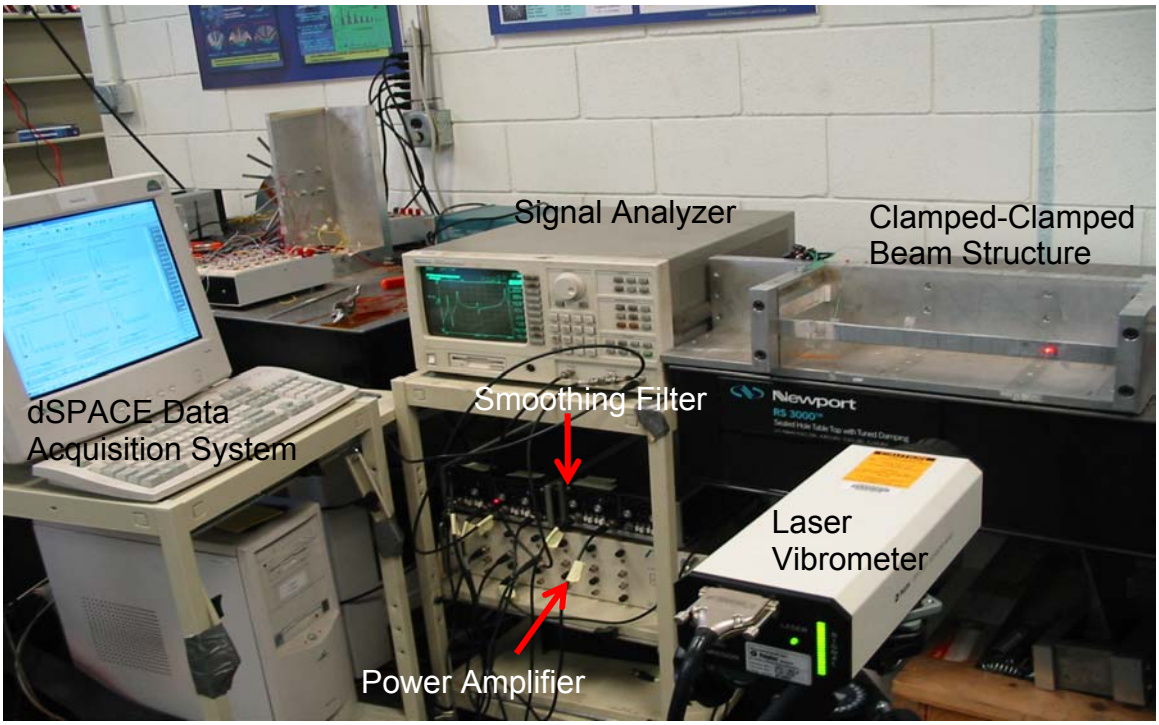

Figure **4-1**: Photograph of experimental setup

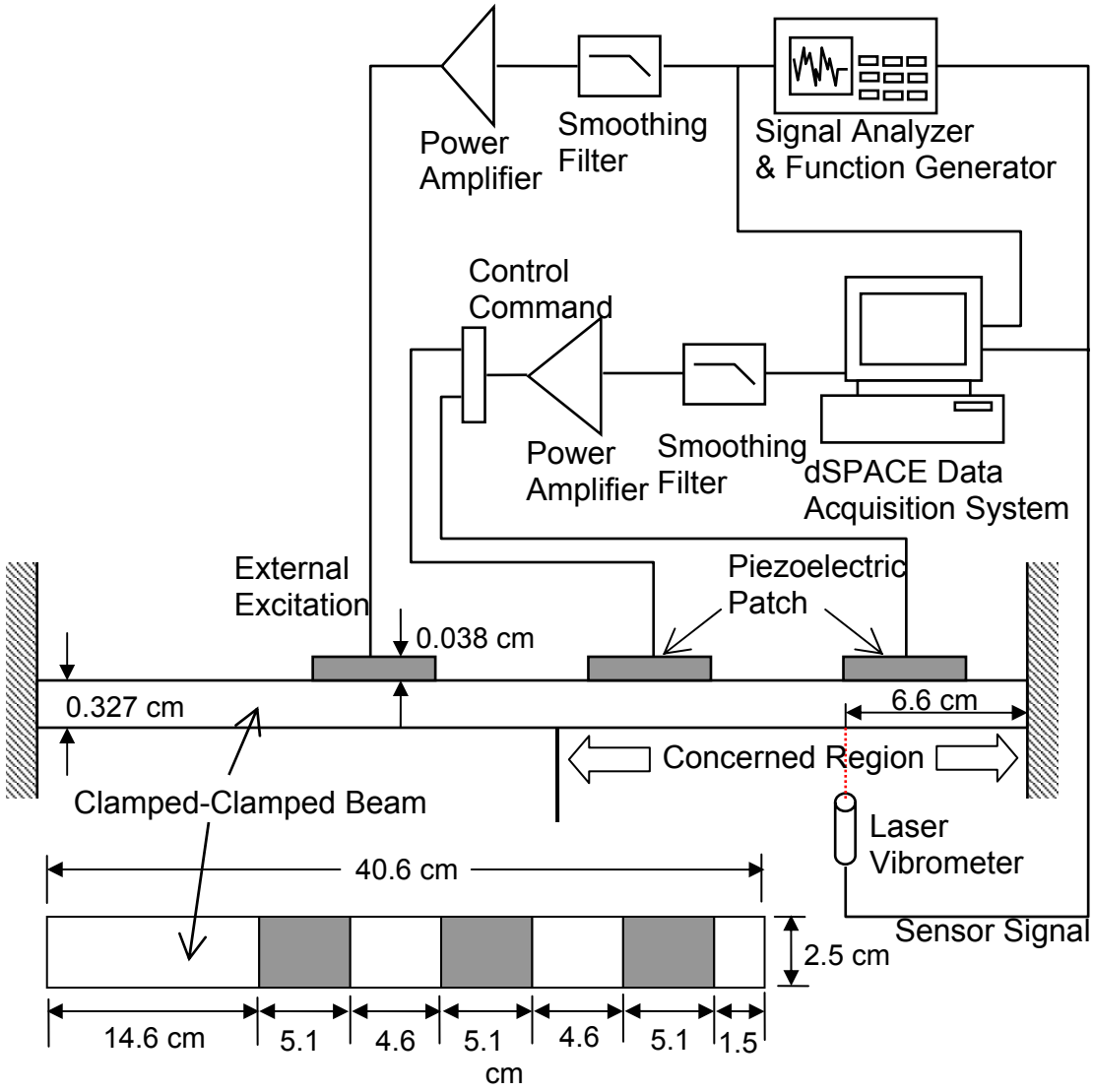

Figure **4-2**: Schematic of experimental setup

As shown in Figure **4-2**, three piezoelectric patches are bonded on the top surface of the host beam structure. The left patch is used as an external exciter and the other two are used as actuators (control inputs) for active control. The concerned region is selected to be the right half part of the beam. A Non-contact laser vibrometer sensor is utilized to

measure the structural velocity at the position shown in the figure. A PC-based digital control system, which consists of the SIMULINK software and the dSPACE DS1103 control board, is used to realize the active control laws. A disturbance signal is generated and applied on the left piezoelectric patch as the external excitation. The velocity sensor signal is sent to the A/D converters of the dSPACE board and the data acquisition system. The control signals from the D/A converters of the dSPACE board are filtered and amplified, and then fed to the piezoelectric actuators.

4.3 System Identification

As described in the previous chapters, an accurate system model is required before the left and right eigenvector assignment method can be applied. It is in general difficult to obtain a discretized analytical model which can precisely describe all the physical characteristics of the actual continuous structure. The uncertainties in the experimental setup will also reduce the accuracy of the system model that is to be used for controller design. Therefore, in many applications, system identification techniques are utilized to experimentally characterize the system mathematical model. The conventional system identification techniques, such ARX and ARMAX (Ljung, **1999**), requires high-order models to approximate the system such that an acceptable mathematical model can be obtained, which may cause numerical difficulties and is very inefficient. To compromise this dilemma, the experimental modal analysis technique

combined with the structured state-space parameterization algorithm is utilized in this investigation to derive the system state model.

The experimental modal analysis is a well known test method for determining the structure's natural frequencies, damping ratios and mode shapes. This therefore will be performed in the first step of model identification. Considering the integrated clamped-clamped beam structure with piezoelectric patches as shown in Figure **4-2**, the system mathematical model, Equation **2.25**, can be transformed into the modal space expression by substituting $q=\Phi\mathsf{h}$ and pre-multiplying Φ^T on each term of Equation **2.25**, i.e.

$$\Phi^T M\Phi\ddot{\eta}+\Phi^T C_d\Phi\dot{\eta}+\Phi^T K_{eq}\Phi\eta=\Phi^T F_d f+\Phi^T B_{eq}V \qquad (4.1)$$

where Φ is the right eigenvector matrix and h is the modal coordinate vector. Since the system is light-damped, we can assume that the system model can be decoupled to a diagonal form by properly scaling Φ, i.e.

$$\ddot{\eta}+\begin{bmatrix}\ddots & & 0\\ & \zeta_j\omega_j & \\ 0 & & \ddots\end{bmatrix}\dot{\eta}+\begin{bmatrix}\ddots & & 0\\ & \omega_j^2 & \\ 0 & & \ddots\end{bmatrix}\eta=F_m f+B_m V \qquad (4.2)$$

where $F_m=\Phi^T F_d$ and $B_m=\Phi^T B_{eq}$. Therefore the state space form can be expressed in terms of the modal coordinates,

$$x=\begin{Bmatrix}\eta\\ \dot{\eta}\end{Bmatrix},\quad A=\begin{bmatrix}0 & & I & \\ \ddots & & \ddots & \\ -\omega_j^2 & & -\zeta_j\omega_j & \\ & \ddots & & \ddots\end{bmatrix},\quad B=\begin{bmatrix}0\\ F_m\end{bmatrix},$$
$$C=\begin{bmatrix}0 & C_o\Phi\end{bmatrix},\quad E=\begin{bmatrix}0\\ B_m\end{bmatrix} \qquad (4.3)$$

where C_o is a Boolean row vector representing measured output. The natural frequencies ω_j, damping ratios ζ_j and mode shapes ϕ_j (right eigenvector) of the structure can be determined by the STAR MODAL software from the experimental data through the modal analysis technique. Therefore the matrices A and C of state space format in Equation **4.3** can be modeled in term of the damping ratios ζ_j, natural frequencies ω_j, and right eigenvectors ϕ_j.

In the state space format of Equation **4.3**, matrices A and C are fixed while the elements in the bottom half of B and E can be freely adjusted. In such a structured-matrices condition, one can utilize the structured state-space parameterization algorithm (Ljung, **1999**) to determine the parameters F_m and B_m (or F_d and B_{eq}) in Equation **4.3**. The structured state-space parameterization algorithm can be executed by the MATLAB System Identification Toolbox.

The frequency bandwidth is selected to be 800 Hz in the experiments. Within the bandwidth, four vibration modes of the test stand can be detected. Table **4-1** shows the results of experimental modal analysis, which includes the damping ratios, natural frequencies and mode shapes.

Table **4-1**: Results of experimental modal analysis

	1st Mode	2nd Mode	3rd Mode	4th Mode
Damping Ratio z_j (%)	0.6757	0.6770	0.2804	0.3843
Natural Frequency w_j (Hz)	94.0267	224.6200	449.6700	761.0467
Eigenvalue λ_j	-3.9919 ≤590.7735i	-9.5545 ≤1411.2967i	-7.9224 ≤2825.3488i	-18.3752 ≤4781.7619i
Mode Shape f_j	7.1621 +12.8257i	11.8351 +30.7512i	13.4880 +22.5547i	4.3903 +12.3636i
	28.8294 +18.9346i	18.8823 +10.7747i	-10.3232 -3.7213i	-16.7612 -17.8331i
	-276.1478 +4.1180i	98.5884 -1.0658i	74.2546 -0.2617i	-172.3970 -20.8879i
	92.5224 -204.3723i	-92.6700 +206.4647i	51.7835 -105.3933i	-76.6960 +96.3050i

Since the structure is lightly damped, the following rule can be used to convert complex modes to real modes in STAR MODAL. All complex modal coefficients which have phase between -67.5˚ and 112.5˚ are changed to 0˚ and all other complex modal coefficients are changed to 180˚. Figure **4-3** shows the mode shapes of the first four modes of the structure with real modal coefficients. Point 1 to 4 are the measured points in the modal analysis process and point 0 and 5 are fixed points at the clamped ends.

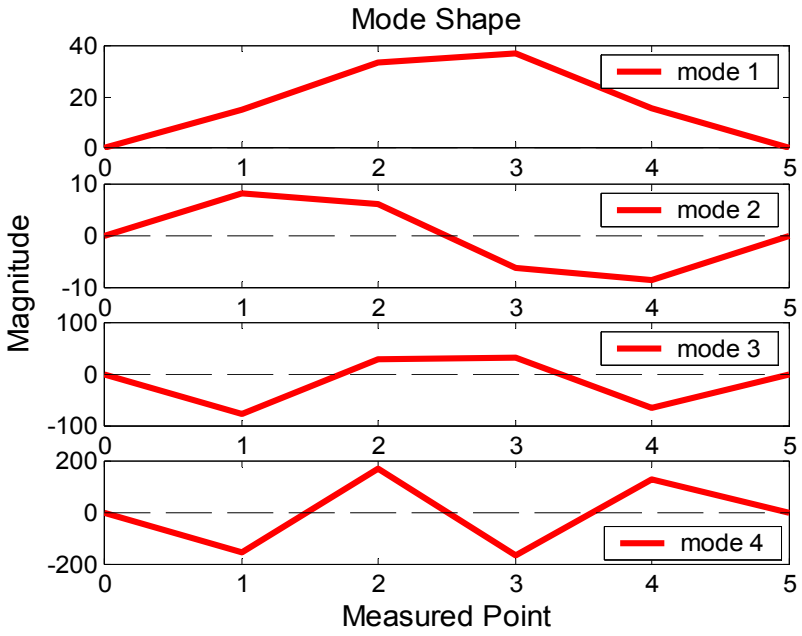

Figure 4-3: Mode shapes of first four modes with real modal coefficients

Through the structured state-space parameterization process and coordinate transformation, the state space model with displacement/velocity state vector can be obtained as described in Equation **4.4**. Figure **4-4** to Figure **4-6** show the frequency response functions of velocity sensor signal to the first, second actuator inputs and excitation signals, respectively. The errors between measured data and identified model are mainly caused due to the assumption that the system model can be perfectly decoupled to a diagonal form as Equation **4.3**.

$$A=\begin{bmatrix} 0 & 0 & 0 & 0 & 1 & 0 & 0 & 0 \\ 0 & 0 & 0 & 0 & 0 & 1 & 0 & 0 \\ 0 & 0 & 0 & 0 & 0 & 0 & 1 & 0 \\ 0 & 0 & 0 & 0 & 0 & 0 & 0 & 1 \\ -8.62\times10^{6} & 7.21\times10^{6} & -4.11\times10^{6} & 1.97\times10^{6} & -20.2213 & 6.4404 & -3.6495 & 6.2979 \\ 5.91\times10^{6} & -8.36\times10^{6} & 6.56\times10^{6} & -3.81\times10^{6} & 5.2724 & -19.9954 & 10.1078 & -2.9617 \\ -2.95\times10^{6} & 6.76\times10^{6} & -8.11\times10^{6} & 6.57\times10^{6} & -2.2235 & 10.6488 & -19.2654 & 5.8020 \\ 1.31\times10^{6} & -3.86\times10^{6} & 6.26\times10^{6} & -8.09\times10^{6} & 5.0540 & -2.5942 & 5.5113 & -20.2057 \end{bmatrix}$$

$$B=\begin{bmatrix} 0 & 0 \\ 0 & 0 \\ 0 & 0 \\ 0 & 0 \\ -178.0685 & 1.6444\times10^{2} \\ 197.8725 & -2.9724\times10^{2} \\ -77.2575 & 2.6050\times10^{2} \\ 40.1966 & -1.3339\times10^{2} \end{bmatrix}$$

$$C=\begin{bmatrix} 0_{1\times4} & 1 & 0 & 0 & 0 \end{bmatrix} \qquad (4.4)$$

$$E=\begin{bmatrix} 0 \\ 0 \\ 0 \\ 0 \\ -24.1282 \\ 153.2090 \\ -293.8711 \\ 189.0922 \end{bmatrix}$$

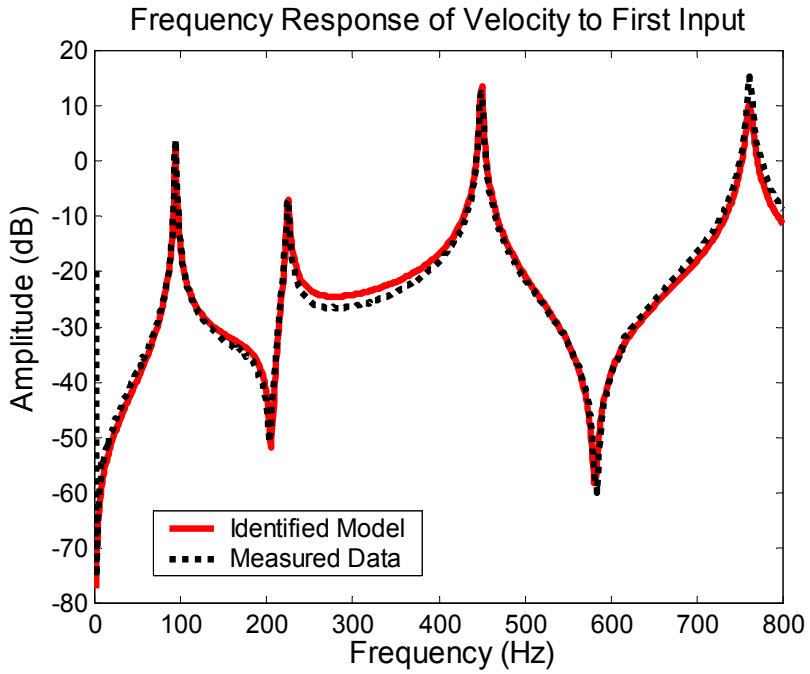

Figure 4-4: Frequency response function of velocity sensor to first input signal.

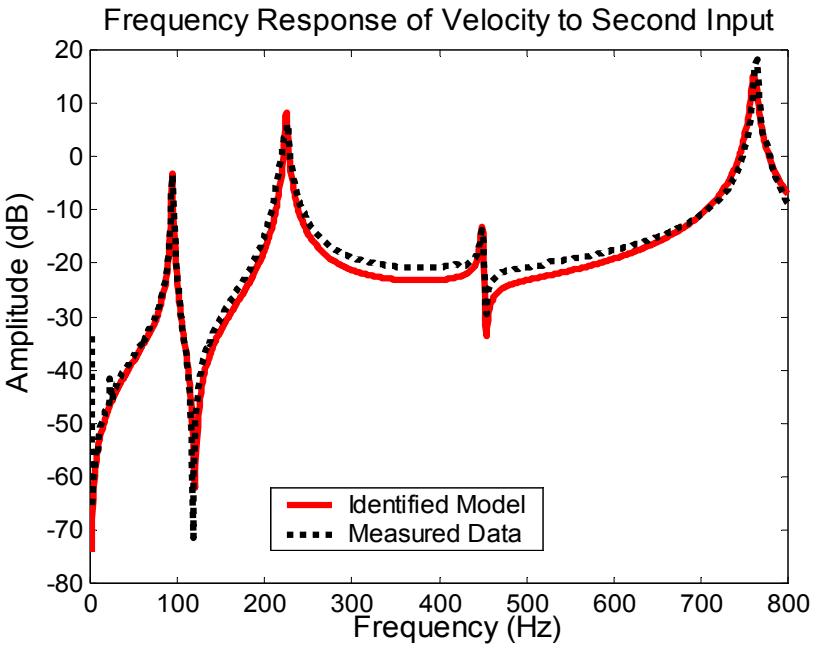

Figure 4-5: Frequency response function of velocity sensor to second input signal.

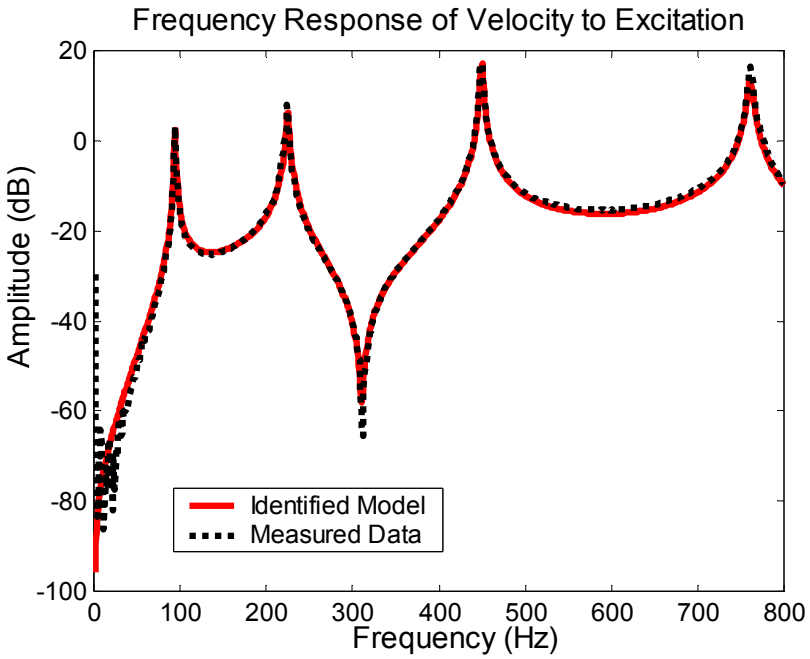

Figure 4-6: Frequency response function of velocity sensor to excitation signal.

4.4 State Estimator

The simultaneous left-right eigenvector assignment algorithm discussed in Chapter 2 is derived based on the full state feedback assumption so that the closed-loop eigenvalues can be exactly located. In Chapter 3, even though the partial left-right eigenvector assignment algorithm is developed in an output feedback configuration, the required number of outputs is generally greater than the number of measurements in the practical situation. Therefore, a state estimator is required for implementation of the left-

right eigenvector assignment algorithms in the experiments. In this section, the state estimator will be introduced to estimate the unmeasured states. The block diagram of the integrated system with the state estimator is shown in Figure **4-7**.

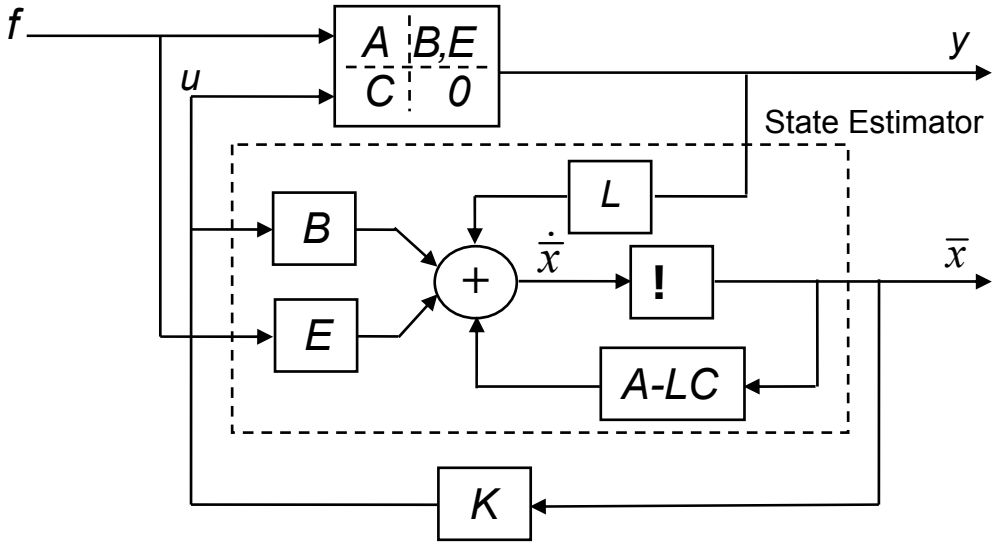

Figure **4-7**: Block diagram of the integrated system with state estimator

The equation of the state estimator is written as

$$\dot{\bar{x}} = (A - LC)\bar{x} + Bu + Ef + LCx \qquad (4.5)$$

where $\bar{x}$ is the estimated state vector and L is the output gain matrix to be decided. By separation property (Chen, **1984**), the design of state feedback and the design of the state estimator can be carried out independently and the eigenvalues of the entire system are the union of those of state feedback and those of the estimator. Combining the equations

of the state feedback system, Equation **2.1**, and the state estimator, Equation **4.5**, the closed-loop system thus becomes

$$\begin{Bmatrix} \dot{x} \\ \dot{\bar{x}} \end{Bmatrix} = \begin{bmatrix} A & BK \\ LC & A-LC+BK \end{bmatrix} \begin{Bmatrix} x \\ \bar{x} \end{Bmatrix} + \begin{bmatrix} E \\ E \end{bmatrix} f$$
$$y = \begin{bmatrix} C & 0 \end{bmatrix} \begin{Bmatrix} x \\ \bar{x} \end{Bmatrix} \qquad (4.6)$$

4.5 Controller Design

In the experiment, the state vector of the discretized state space model in Equation **2.1** represents the displacements and velocities of the four points on the beam structure. The concerned region is selected to be the two right points of the beam structure as shown in Figure **4-2**. Therefore the Boolean matrix in Equation **2.19** is expressed as

$$b = \begin{bmatrix} 1 & 0 & 0 & 0 & 0 & 0 & 0 & 0 \\ 0 & 1 & 0 & 0 & 0 & 0 & 0 & 0 \\ 0 & 0 & 0 & 0 & 1 & 0 & 0 & 0 \\ 0 & 0 & 0 & 0 & 0 & 1 & 0 & 0 \end{bmatrix} \qquad (4.7)$$

and the one in Equation **3.18** is described as

$$b = \begin{bmatrix} 1 & 0 & 0 & 0 & 0 & 0 & 0 & 0 \\ 0 & 1 & 0 & 0 & 0 & 0 & 0 & 0 \\ 0 & 0 & 0 & 0 & 0 & 0 & 0 & 0 \\ 0 & 0 & 0 & 0 & 0 & 0 & 0 & 0 \\ 0 & 0 & 0 & 0 & 1 & 0 & 0 & 0 \\ 0 & 0 & 0 & 0 & 0 & 1 & 0 & 0 \\ 0 & 0 & 0 & 0 & 0 & 0 & 0 & 0 \\ 0 & 0 & 0 & 0 & 0 & 0 & 0 & 0 \end{bmatrix} \quad (4.8)$$

Through the simultaneous and partial left-right eigenvector assignment algorithms developed in Chapter 2 and Chapter 3, one can solve for the feedback gain matrices for the identified state space model in Equation **4.4**.

To determine the feedback gain matrix of the simultaneous left-right eigenvector assignment algorithm, the performance prediction index (as defined in Equation **2.30)** versus weighting factor ratio is first calculated and shown in Figure **4-8**.

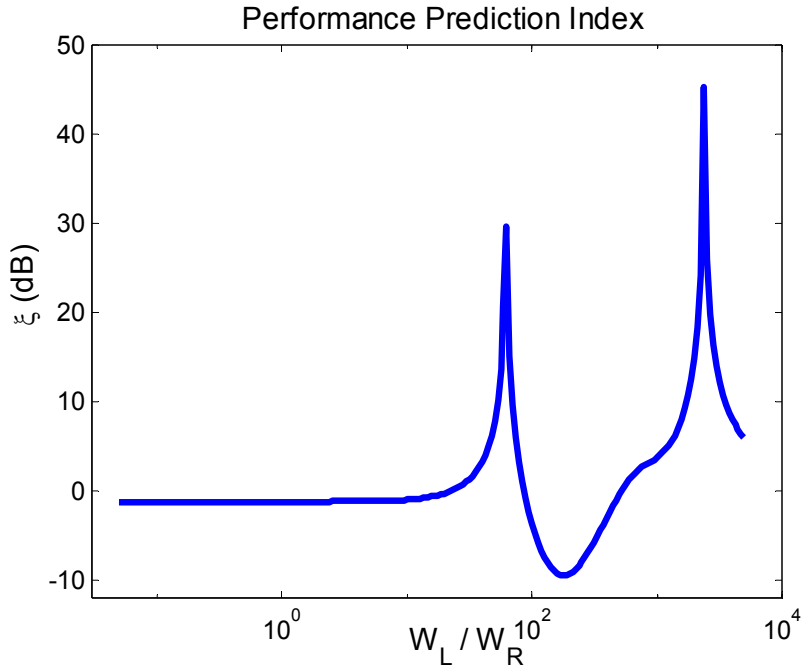

Figure **4-8**: Performance prediction index vs. weighting factor ratio for the identified model.

The minimal (best) performance prediction index for this identified model is obtained at w_L/w_R=177.407. The feedback gain matrix for the identified model is thus determined (Equation **2.23**) as

$$K = \begin{bmatrix} -1.95\times10^{5} & -1.37\times10^{5} \\ 8.33\times10^{4} & 2.53\times10^{4} \\ -3.69\times10^{4} & -1.00\times10^{4} \\ 1.73\times10^{4} & -0.33\times10^{4} \\ -16.274 & -25.553 \\ 170.836 & 138.760 \\ 37.054 & 29.954 \\ 30.427 & 25.366 \end{bmatrix}^{T} \qquad (4.9)$$

For the partial left-right eigenvector assignment algorithm, the output number is selected to be seven. In this case, the right eigenvectors at the first, second and fourth modes are first assigned and then followed by assigning the left eigenvectors of the third mode (447.361 Hz). The feedback gain matrix (Equation **3.15**) in this case is determined as

$$K = \begin{bmatrix} 7.90\times10^{4} & 7.79\times10^{4} \\ 2.14\times10^{5} & 1.44\times10^{5} \\ -2.98\times10^{4} & -0.71\times10^{4} \\ 5.80\times10^{4} & 4.03\times10^{4} \\ 54.3469 & 46.1825 \\ 52.8336 & 49.2237 \\ 0.7756 & 1.3601 \end{bmatrix}^{T} \qquad (4.10)$$

The output gain of state estimator L in Equation **4.5** for both methods is also determined to be

$$L = \begin{bmatrix} -2.2579 \\ 6.0280 \\ 2.0691 \\ 3.3218 \\ 13219.8235 \\ 4282.1373 \\ 1279.2240 \\ 1281.4294 \end{bmatrix} \qquad (4.11)$$

4.6 Modified Feedforward Configuration

For the experimental test stand, the identified frequency response functions consist of not only the mechanical structure dynamics, but also the dynamics of the velocity sensor, low pass filters and power amplifiers. All the components will increase the damping effects of the loop characteristics. It will reduce the precision of the identified state space model if the complex modal coefficients are converted to real modal coefficients. Under this circumstance, the closed-loop feedback system with state estimator may not tolerate the discrepancy between the identified model and the actual system. That will cause instability or unsatisfactory performance.

In order to address this issue, a modified feedforward configuration is proposed in this section to decrease the effects of system uncertainties and undesired noise. The block diagram of the modified feedforward configuration is shown in Figure **4-9**. In the schematic, f is the external excitation, y is the structural velocity measured by the laser vibrometer sensor, u is the control voltage input activated by the dSPACE system, and x represents the state vector of the identified state space model. As shown in this figure, the control input u applied to the actuators is determined from the product, Kx, in which the feedback gain matrix K is the same as that determined in Equation **4.9** or Equation **4.10**, and the state x is determined from the output of the identified state-space model, instead of the state vector output of the state estimator as shown in Figure **4-7**.

With such a modified configuration, the system instability caused from the sensor noise can be relaxed so that the feedforward system is more robust against the uncertainties and undesired noise.

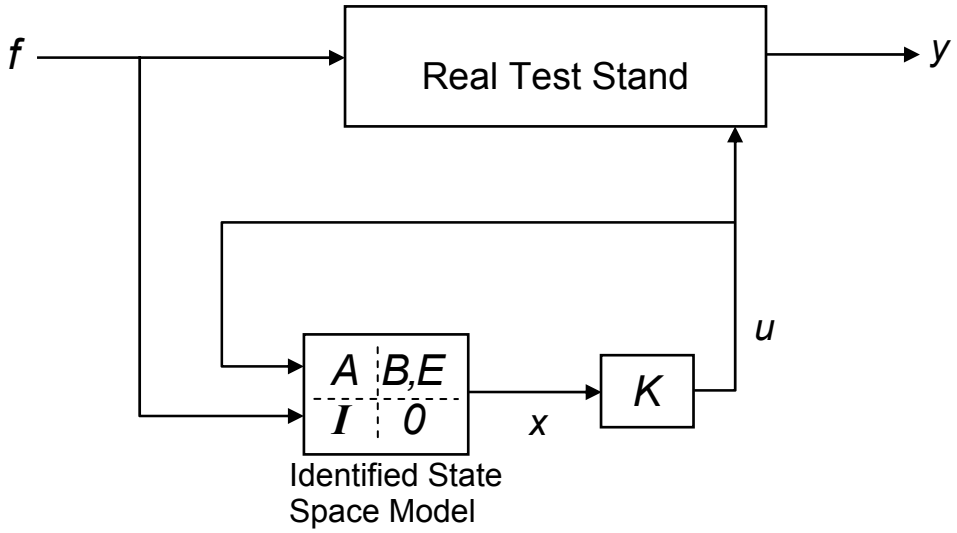

Figure 4-9: Modified feedforward configuration

The experimental results are shown in Figure **4-10** and Figure **4-11**. These two figures show the frequency responses of the measured velocity to the external excitation with and without applying the left-right eigenvector assignment methods. By applying the simultaneous left-right eigenvector assignment method or the partial left-right eigenvector assignment algorithm, the vibration amplitude at the measured point (in the concerned region) can be well suppressed (up to 15 dB) at the resonant frequencies.

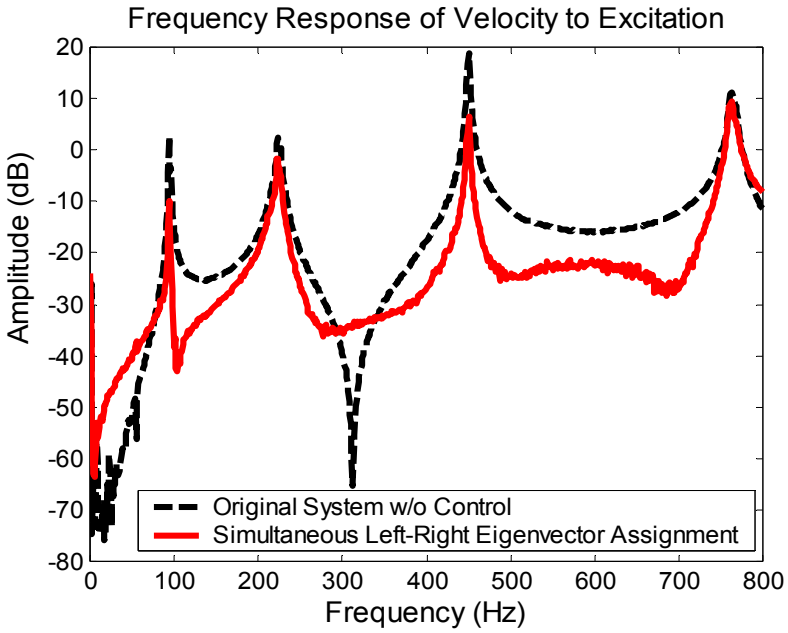

Figure 4-10: Frequency response of velocity sensor to excitation signal w/ and w/o simultaneous left-right eigenvector assignment method

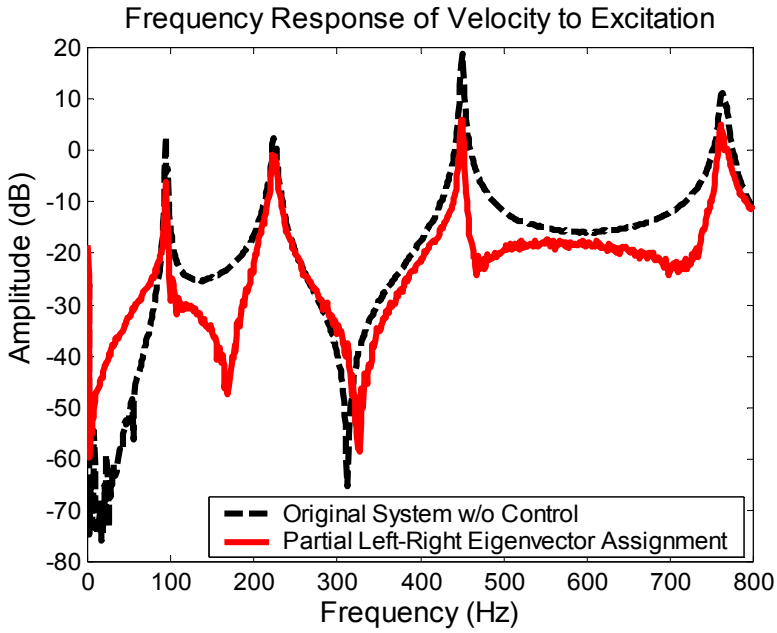

Figure 4-11: Frequency response of velocity sensor to excitation signal w/ and w/o partial left-right eigenvector assignment method

4.7 Summary

An experimental investigation is performed to validate the proposed left-right eigenvector assignment algorithms for vibration control. The test stand hardware, including a piezoelectric transducer integrated beam structure, smoothing filters, power amplifiers, signal analyzer and function generator, and PC-based dSPACE data acquisition system, is set up to implement the control laws. A system identification process consisting of experimental modal analysis and structured state-space parameterization is introduced. A modified feedforward configuration is utilized to accommodate for the system uncertainties and undesired noise so that both the simultaneous left-right eigenvector assignment and partial left-right eigenvector assignment algorithms can be implemented. The experimental results show that both the proposed approaches can be implemented and achieve vibration suppression.

Chapter 5

REDUCTION OF STRUCTURAL ACOUSTIC RADIATION VIA LEFT-RIGHT EIGENVECTOR ASSIGNMENT

5.1 Introduction

The objective of the research study in this chapter is to expand the concept of the left and right eigenvector assignment developed in Chapter 2 and Chapter 3 and achieve structural acoustic radiation control. Many studies have been conducted in the field of active control of sound. In the traditional active noise control (ANC) methods, destructive interference is normally applied by other acoustic sources to reduce the sound pressure field (Nelson and Elliott, **1992**; Fuller and von Flotow, **1995**; Bai and Wu, **1997**). On the other hand, the active structural acoustic control (ASAC) concept has also attracted much attention, where the radiated sound pressure is attenuated by directly applying active actions to the structure rather than by exciting the medium with acoustic sources (Clark and Fuller, **1992**). With the ASAC technique, sensors and actuators are integrated in the structure to form a compact, smart and quiet system, thus the numerous acoustic sources and error signal microphone necessary in the classical ANC system are not required (Maillard and Fuller, **1999**).

A state-space, model-based ASAC method has been investigated by Meirovitch and Thangjitham (Meirovitch and Thangjitham, **1990;** Meirovitch and Thangjitham, **1990**). Their approach is based on vibration control of harmonic disturbances, with observation of resulting far-field radiated pressure during the tuning process of vibration cost function. Alternatively, previous research works investigated the ASAC problem using quadratic optimization techniques to determine the required control forces and moments on the structure that will minimize the radiated acoustic power (Fuller, **1990**; Naghshineh and Koopmann, **1994**; Lee and Park, **1996**; Sung and Jan, **1997**). The structurally radiated noise can also be formulated as the standard LQR (linear quadratic regulator) and LQG (linear quadratic Gaussian) problems, and the active feedback system can suppress the structural radiated sound pressure that is included within the cost function expression (Baumann et al., **1991**; Baumann et al., **1992**; Sung and Chiu, **1997**; Dehandschutter et al., **1999**).

To advance the state of the art in ASAC, the research in this chapter is to explore the feasibility of utilizing the left and right eigenvector assignment methods for active control of structural acoustic radiation. Since both left and right eigenvectors are physically meaningful to the system dynamics, this approach will directly target the nature of vibrating structure. In this chapter, a new assigning strategy of right eigenvectors is derived so that the modal velocity distributions are shaped through solving a generalized eigenvalue problem, where the modal radiation is minimized. Combining the design criteria of left eigenvector assignment, one can achieve disturbance rejection and mode shape tailoring concurrently so that the structural sound radiation can be reduced.

In the next section, the mathematical model of structural sound pressure radiation will be first discussed. The shaping strategy of modal velocity distribution is also derived. Numerical simulations are then performed to evaluate the effectiveness of the simultaneous left-right eigenvector assignment and partial left-right eigenvector assignment methods for structural acoustic control.

5.2 Modeling of Structural Acoustic Radiation

Figure **5-1** shows a schematic of the vibrating clamped-clamped beam structure as illustrated in Chapter 2 and Chapter 3. A microphone receiver is placed to detect the noise signal as shown in the figure.

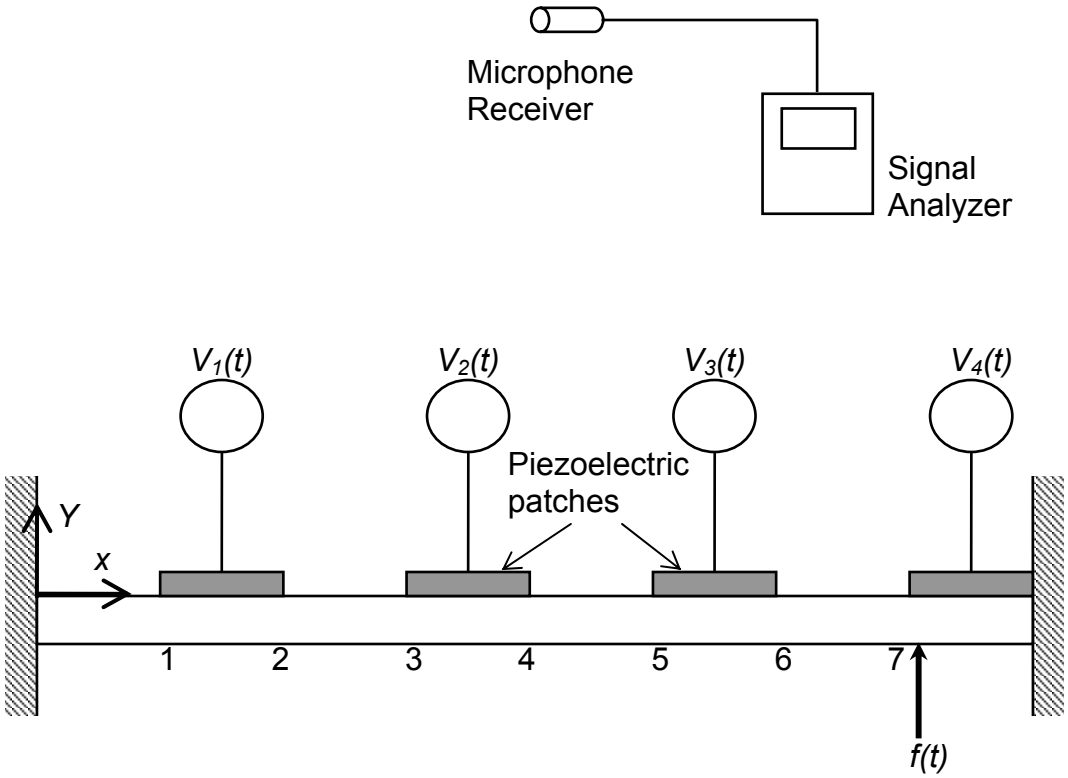

Figure 5-1: System arrangement consisting host clamped-clamped beam, piezoelectric patches, and active control voltage inputs. External disturbance is exerted on point 7. A microphone receiver is placed to detect the noise signal.

The discretized equations of motion for the integrated system can be also expressed as Equation **2.25** and transformed to state space form as Equation **2.1** or Equation **3.1**. The radiated acoustical pressure can be described as a function of the structural vibration profile. For flat sources, the radiated sound pressure at the observation position $\vec{R}$ in the medium can be described by the Rayleigh integral (Blackstock, **2000**), which is a general expression as a surface integral of the normal surface velocity on the planar structure, i.e.

$$P(\vec{R},\omega)=\frac{i\omega\rho_a}{2\pi}\iint_S V_n(\vec{r}_s)\frac{e^{-ik\left|\vec{R}-\vec{r}_s\right|}}{\left|\vec{R}-\vec{r}_s\right|}dS \tag{5.1}$$

where $V_n(\vec{r}_s)$ is the velocity in the direction normal to the vibrating surface of structure at the position $\vec{r}_s$, ρ_a is the medium density, w is the structural vibration frequency, the wave number k=w/C_a and C_a is the sound speed in the medium. We define

$$h_j=\frac{i\omega\rho_a\Delta S_j}{2\pi\left|\vec{R}-\vec{r}_{sj}\right|}e^{-i\frac{\omega}{C_a}\left|\vec{R}-\vec{r}_{sj}\right|} \tag{5.2}$$

and

$$H=\left[0_{1\times n}\,|\,h_1\ 0,h_2\ 0,...,h_n\ 0\right] \tag{5.3}$$

The expression of radiated sound pressure at the observation point in the medium can thus be formulated in terms of the state equation solution, i.e.

$$P=Hx(t)=H\Phi\int_0^t e^{\Lambda(t-\tau)}\Psi^T Ef(\tau)d\tau \tag{5.4}$$

where Λ is a diagonal matrix including the eigenvalues of the closed-loop system, Φ and Ψ are the corresponding right and left eigenvector matrices, respectively. It is clear, from Equation **5.4**, that the radiated sound pressure depends on both the right eigenvectors (mode shape concept) and left eigenvectors (disturbance rejection concept). The goal of this research, therefore, is to alter both the left and right eigenvectors by applying active feedback action so that the radiated sound pressure can be minimized.

5.3 Left-Right Eigenvector Assignment Algorithm for Reduction of Structural Acoustic Radiation

Both simultaneous left-right eigenvector assignment and partial left-right eigenvector assignment methods will be applied for reducing the structural sound radiation. Since the concept of left eigenvector assignment for noise control is also to enhance the system capability of disturbance rejection, the design strategy of left eigenvectors will be the same as that given in **2.2** and **3.3.1**. Reciprocally, the design criterion of right eigenvectors for noise reduction is different from that for vibration control and will thus be introduced in the following section.

5.3.1 Right Eigenvector Assignment: Modal Velocity Tailoring

The idea of using right eigenvector assignment for structural noise reduction is to alter the right eigenvectors such that the profile of modal velocity distribution will cause minimum acoustic radiation. In the sense of far-field sound pressure, the velocity

distribution in the normal direction of the vibrating surface should be as asymmetrical as possible. In this study, we define

$$q_{jk} = \frac{i\omega_j \rho_a \Delta S_k}{2\pi \left| \vec{R} - \vec{r}_{sk} \right|} e^{-i\frac{\omega_j}{C_a}\left|\vec{R}-\vec{r}_{sk}\right|} \quad j = 1,\ 2,...,\ 2n\ ;\ k = 1,\ 2,...,\ n \tag{5.5}$$

where ω_j is the jth resonant frequency corresponding to the assigned right eigenvector, $\vec{r}_{sk}$ is the kth position vector on the vibrating surface. Define D_j to be the jth modal velocity vector, which is the sub-vector of the jth right eigenvector including all the modal velocity components in the normal direction:

$$D_j = \left[d_{j1},\ d_{j2},...,\ d_{jn} \right]^T,\ j = 1,\ 2,...,\ 2n \tag{5.6}$$

For noise radiation reduction purpose, we define the modal radiation index of the jth mode, ξ_j to be

$$\xi_j = \frac{(Q_j^T D_j)^2}{\left\| Q_j \right\|_2^2 \left\| D_j \right\|_2^2} + \frac{(Q_j^T D_j^*)^2}{\left\| Q_j \right\|_2^2 \left\| D_j^* \right\|_2^2},\ j = 1,\ 2,...,\ 2n \tag{5.7}$$

where $Q_j = \left[q_{j1},\ q_{j2},...,\ q_{jn} \right]^T$. Based on the Rayleigh integral in Equation **5.4**, it is desirable to minimize ξ_j so that the sound radiation from the vibrating structure can be

reduced. Therefore we can formulate this idea by substituting Equation **2.10** (or Equation **3.5**) into Equation **5.7**,

$$\begin{aligned}\min \xi_j &= \min_{\mu_j}\left(\frac{\mu_j^* v_j'^* (\bar{Q}_j Q_j^T) v_j' \mu_j}{\mu_j^* (\|Q_j\|_2^2 v_j'^* v_j') \mu_j} + \frac{\mu_j^T v_j'^T (\bar{Q}_j Q_j^T) \bar{v}_j' \bar{\mu}_j}{\mu_j^T (\|Q_j\|_2^2 v_j'^T \bar{v}_j') \bar{\mu}_j}\right) \\ &= \min_{\mu_j}\left(\frac{\mu_j^* (2 v_j'^* \bar{Q}_j Q_j^T v_j') \mu_j}{\mu_j^* (\|Q_j\|_2^2 v_j'^* v_j') \mu_j}\right) = \alpha_{j,\min}\end{aligned} \tag{5.8}$$

where v_j' is the sub-matrix of the jth right eigenvector subspace v_{j2} in Equation **2.10** (or Equation **3.5**), including the modal velocity components in the normal direction, and $(\bar{\bullet})$ denotes the complex conjugate of (•). The design criterion for the closed-loop right eigenvectors is thus to determine the vector μ_j so that ξ_j is minimized. Let

$$\begin{aligned}F_j &= 2 v_j'^* \bar{Q}_j Q_j^T v_j' \\ J_j &= \|Q_j\|_2^2 v_j'^* v_j'\end{aligned} \tag{5.9}$$

The optimal solution μ_j in Equation **5.8** is equivalent to the eigenvector corresponding to the minimal eigenvalue $\alpha_{j,min}$ among all eigenvalues α_j in the generalized eigenvalue problem:

$$F_j \mu_j = \alpha_j J_j \mu_j \tag{5.10}$$

The desired right eigenvectors for structural noise control purpose are thus obtained as

$$\phi_j^d = v_{j2}\mu_j, j = 1,2,...,N \tag{5.11}$$

5.3.2 Simultaneous Left-Right Eigenvector Assignment Algorithm

As aforementioned that the desired left eigenvectors for disturbance rejection can be obtained by Equation **2.12** to Equation **2.15**, the optimal desired left eigenvectors are thus determined by minimizing the orthogonality indices as

$$\Psi^d = \left[v_{12}^{(L)}\gamma_1, v_{22}^{(L)}\gamma_2, ..., v_{N2}^{(L)}\gamma_N \right] = \left[\psi_1^d, \psi_2^d, ..., \psi_N^d \right] \tag{5.12}$$

where γ_j is the eigenvector corresponding to the minimal eigenvalue of the generalized eigenvalue problem in Equation **2.15**.

Therefore the simultaneous left-right eigenvector assignment approach can be formulated by substituting Equation **5.11** and Equation **5.12** into Equation **2.20** and minimizing the performance index, i.e.

$$J_j = \min_{\mu_j} \left\| \begin{bmatrix} w_L (\Psi^d)^T v_{j2}^{(R)} \\ w_R v_{j2}^{(R)} \end{bmatrix} \{\mu_j\} - \begin{Bmatrix} w_L I_j \\ \phi_j^d \end{Bmatrix} \right\|^2, \quad j = 1,2,...,N \tag{5.13}$$

where w_L and w_R are the weighting factors on the left and right eigenvectors respectively, ϕ_j^d is the desired right eigenvector for structural noise reduction derived in Equation **5.11**. The optimal solution of Equation **5.13** can be determined by letting $dJ_j/d\mu_j=0$, that

$$\tilde{\mu}_j = \left(\begin{bmatrix} w_L (\Psi^d)^T v_{j2}^{(R)} \\ w_R v_{j2}^{(R)} \end{bmatrix}^* \begin{bmatrix} w_L (\Psi^d)^T v_{j2}^{(R)} \\ w_R v_{j2}^{(R)} \end{bmatrix} \right)^{-1} \begin{bmatrix} w_L (\Psi^d)^T v_{j2}^{(R)} \\ w_R v_{j2}^{(R)} \end{bmatrix}^* \begin{Bmatrix} w_L I_j \\ \phi_j^d \end{Bmatrix}, \quad (5.14)$$
$$j = 1, 2, ..., N$$

Substitute $\tilde{\mu}_j$ into Equation **2.10** and Equation **2.4**, we can obtain the following

$$\begin{aligned} \phi_j^a &= v_{j2}^{(R)} \tilde{\mu}_j, \quad \Phi^a = \left[\phi_1^a, \phi_2^a, ..., \phi_N^a \right] \\ w_j &= K \phi_j^a = v_{j4}^{(R)} \tilde{\mu}_j, \quad W = \left[w_1, w_2, ..., w_N \right] \end{aligned} \quad (5.15)$$

where f_j^a is the jth achievable right eigenvector. If the matrix $[\Phi^a B]$ is full rank (Clarke et al., **2003**), then there exists a real feedback gain matrix K that is (Andry et al., **1983**; Kwon and Youn, **1987**)

$$K = W(\Phi^a)^{-1} \quad (5.16)$$

5.3.3 Partial Left-Right Eigenvector Assignment Algorithm

As aforementioned in Chapter 3 that the partial left-right eigenvector assignment algorithm can be divided into two steps, the left eigenvector assignment and the right eigenvector assignment procedures. Either the left or the right eigenvectors are first assigned exactly, and then the achievable subspaces in the second step will be further constrained by imposing the orthogonality condition between the left and right eigenvectors. From the associated achievable subspaces, either in the first step or the second step, both the achievable left and right eigenvectors can be determined as

$$\begin{aligned} \Phi_p^a &= \left[\phi_1^a, \phi_2^a, ..., \phi_p^a\right] = \left[v_{12}\mu_1, v_{22}\mu_2, ...v_{p2}\mu_p\right] \\ \Psi_p^a &= \left[\psi_{p+1}^a, \psi_{p+2}^a, ..., \psi_N^a\right] = \left[m_{p+1,2}\gamma_{p+1}, m_{p+2,2}\gamma_{p+2}, ..., m_{N2}\gamma_N\right] \end{aligned} \tag{5.17}$$

where v_{j2} is the achievable right subspace, m_{j2} is the achievable left subspace, μ_j is determined from Equation **5.10**, γ_j is determined from Equation **3.17**, and p is the number of assigned right eigenvectors. As explained in **3.2**, p cannot be larger than the number of system outputs and (N-p) cannot be larger than the number of system inputs.

From Equation **3.3**, one can determine the following matrices after μ_j and γ_j are solved, i.e.

$$\begin{aligned} W_p &= KC\Phi_p^a = \left[w_1, w_2, ..., w_p\right] = \left[v_{14}\mu_1, v_{24}\mu_2, ...v_{p4}\mu_p\right] \\ Z_p &= K^T B^T \Psi^a = \left[z_{p+1}, z_{p+2}, ..., z_N\right] = \left[m_{p+1,4}\gamma_{p+1}, m_{p+2,4}\gamma_{p+2}, ..., m_{N4}\gamma_N\right] \end{aligned} \tag{5.18}$$

If Φ_p^a and Ψ_p^a satisfy the constraints (a) and (b) of theorem in **3.2**, then the feedback gain matrix is thus obtain (Clarke et al., **2003**) as

$$K = ((\Psi_p^a)^T B)^\dagger Z_p^T + W_p (C\Phi_p^a)^\dagger - ((\Psi_p^a)^T B)^\dagger Z_p^T C\Phi_p^a (C\Phi_p^a)^\dagger \qquad (5.19)$$

where $(\bullet)^\dagger$ denotes the generalized inverse of (∏).

5.4 Numerical Simulations on Reduction of Structural Sound Pressure Radiation

In this section, the clamped-clamped beam structure system shown in Figure **5-1** is used as an example to illustrate the control results and examine the theoretical predictions through numerical simulation. The coordinates (location) of the microphone receiver is X=5.3 m, Y=0.1262 m. The properties of the medium, air, are that temperature is 20°C, density is 1.201 Kg/m^3, and sound speed in the air is 343.400 m/s. All the parameters of the beam structure used in this example are the same as listed in Table **2-1**. The desired closed-loop eigenvalues are the same as the set selected in Chapter 2, which are 5.000 times the real part and 1.006 times the imaginary part of the open-loop eigenvalues.

5.4.1 Case Studies and Analysis: Simultaneous Left-Right Eigenvector Assignment

From Equation **5.7**, the right eigenvector error for structural noise reduction is defined as

$$\varepsilon_R = \sum_{j=1}^{N} \varepsilon_{R_j} = \sum_{j=1}^{N} \left| \frac{2 D_j^{a*} \bar{Q}_j Q_j^T D_j^a}{\left\| Q_j \right\|_2^2 \left\| D_j^a \right\|_2^2} \right| \tag{5.20}$$

where D_j^a is the jth achievable modal velocity vector. On the other hand, the definition of left eigenvector error is the same as in Equation **2.29**. Similarly as in **2.3.4**, one can define the performance prediction index for structural noise reduction as

$$\xi = \sum_{j=1}^{N} \varepsilon_{R_j} \varepsilon_{L_j} \tag{5.21}$$

Figure **5-2** shows the right and left eigenvector errors versus weighting factor ratio w_L/w_R. The overall trend of the two curves indicates that the right eigenvector errors become larger with increasing the weighting factor ratios, while the left eigenvector errors are reduced with increasing the weighting factor ratios.

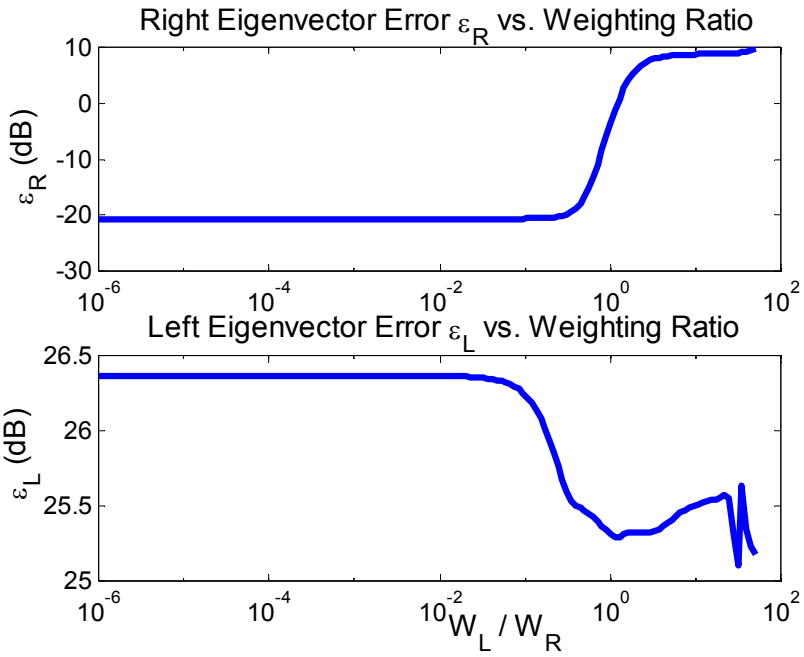

Figure **5-2**: Left and right eigenvector error vs. weighting factor ratio

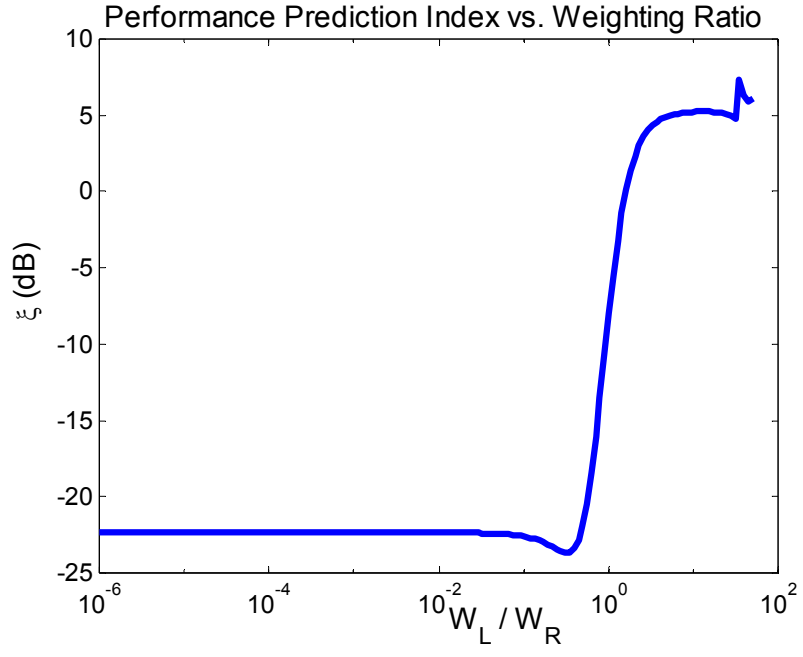

Figure **5-3**: Performance prediction index vs. weighting factor ratio

Figure **5-3** shows the performance prediction index versus weighting factor ratio. The minimal performance prediction index in this example is obtained at w_L/w_R=0.310. The control performance of this case with w_L/w_R=0.310 through the simultaneous left-right eigenvector assignment method is shown as in Figure **5-4**.

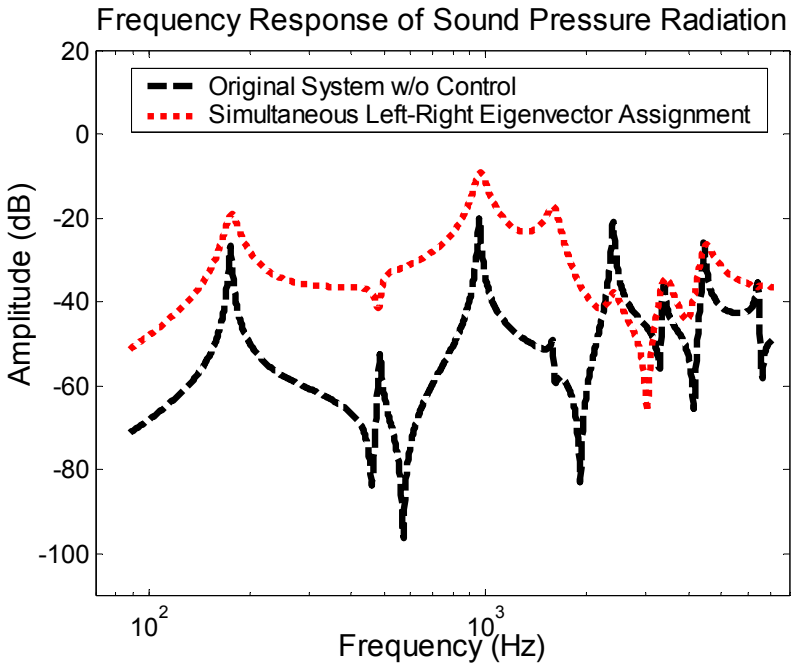

Figure **5-4**: Frequency response of sound pressure radiation at the microphone receiver with w_L/w_R=0.3104.

The sound pressure radiation at the microphone receiver increases through the simultaneous left-right eigenvector assignment method in this case. Although the noise reduction performance is not satisfactory with this weighting factor combination that is determined from performance prediction index, however, from Figure **5-3,** it can be

noticed that the overall trend shows that the performance prediction indices are smaller within very low weighting factor ratios. Based on this observation, one can propose the hypothesis that the right eigenvectors dominates the contribution of the control performance in this case. Therefore it is intuitive to set a lower weighting factor ratio for achieving more obvious suppression. Figure **5-5** shows the frequency response of sound pressure radiation at the microphone receiver with the extreme case, $w_L/w_R=0$, that is pure right eigenvector assignment.

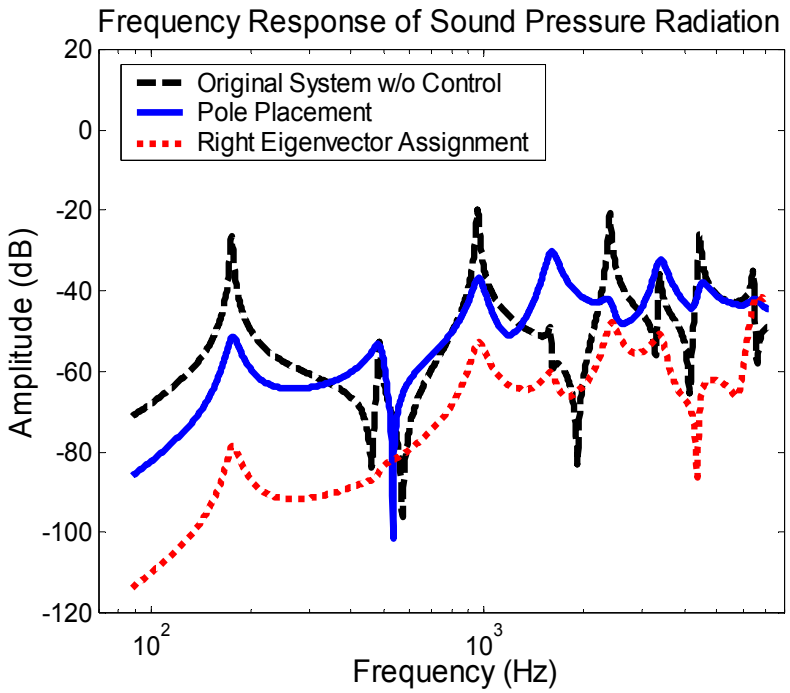

Figure **5-5**: Frequency response of sound pressure radiation at the microphone receiver with $w_L/w_R=0$.

The closed-loop eigenvalues in this example are set the same for both the pole placement and right eigenvector assignment methods. With such a selection, one can

fairly evaluate the further improvement achieved mainly by eigenvector assignment. The result shows that the structural noise radiation can be reduced significantly throughout the broad frequency range by the eigenvector assignment method. It is also noted that both the left and right eigenvectors will be determined based on least square approximation in the simultaneous left-right eigenvector assignment method. However, in this extreme case, all the right eigenvectors can be solved exactly without least square approximation because the desired right eigenvectors are derived from the right achievable subspaces. That is the reason that in this case, the pure right eigenvector assignment method can achieve more structural noise reduction.

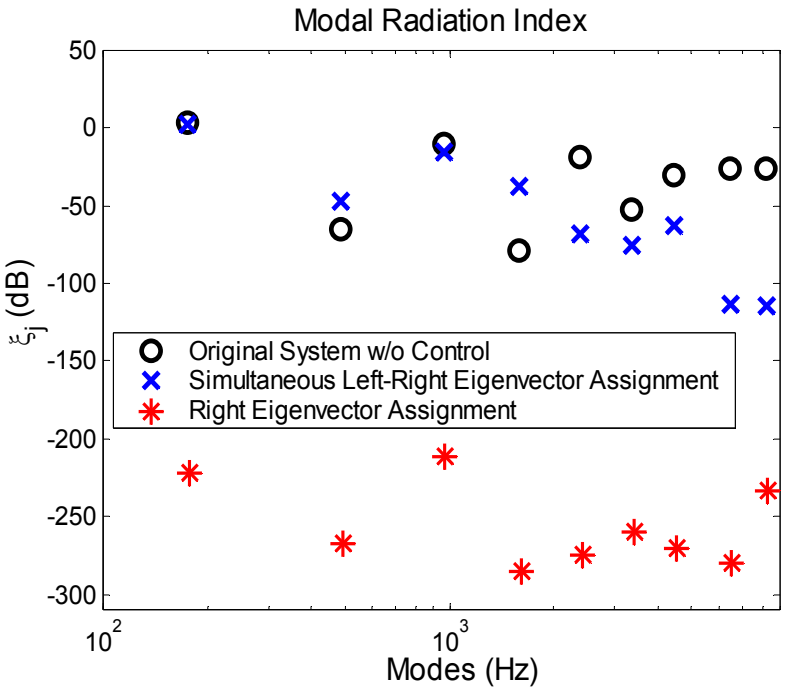

Figure 5-6: Modal radiation index analysis, w_L/w_R=0.3104 and w_L/w_R=0.

Figure **5-6** shows the modal radiation indices of the selected frequency range with cases w_L/w_R=0.310 (simultaneous left-right eigenvector assignment) and w_L/w_R=0 (pure right eigenvector assignment), respectively. Since right eigenvectors are dominant for noise reduction performance in this case, the modal radiation indices have been suppressed more by the pure right eigenvector assignment method than by the simultaneous left-right eigenvector assignment approach.

5.4.2 Case Studies and Analysis: Partial Left-Right Eigenvector Assignment

In this structural acoustic control example, since the same vibrating structure system as in **3.3.2** is used for illustration, the selected two left eigenvectors (a complex conjugate pair) are first assigned and then followed by assigning the remaining (*N-2*) right eigenvectors for the structural noise control purpose.

As depicted in **3.3.2**, it is difficult to evaluate the individual contributions of the left and right eigenvectors independently on the suppression performance at different resonant frequencies. However, the combination number of the total *N* assigned left and right eigenvectors corresponding to the different eigenvalues is limited. Therefore it is easy to select the optimal solution among all the achievable combinations without heavy computational efforts.

Table **5-1** lists the noise reductions at the microphone receiver focused on the first nine resonant frequencies (30-10000 Hz) with all the achievable combinations of the assigned left and right eigenvectors. The left column indicates the first nine resonant peaks and the top row indicates the eigenvalues corresponding to the two left

eigenvectors (complex conjugate pair) which will be first assigned. The middle arrays indicate the frequency response reductions of sound pressure radiation at each resonant frequency with each assigned combination respectively. The smaller magnitude in the middle arrays means more noise suppression. It is determined that the most reduction performance, as shown in the summation row, can be obtained in the shaded case of Table **5-1**.

Table **5-1**: Noise reduction at the microphone receiver at the first 9 resonant frequencies with different combinations of assigned left/right eigenvectors

Eigenvalue / Suppression (dB)	1st Mode -44.0126 ≤ 1106.8805i	7th Mode -1118.7186 ≤ 28134.8733i	8th Mode -1619.8632 ≤ 40738.2556i
1st Resonant Frequency (176.1655 Hz)	-77.5444	-17.9057	-4.1642
2nd Resonant Frequency (488.1796 Hz)	-43.9052	26.3522	36.8562
3rd Resonant Frequency (964.7710 Hz)	-54.3040	0.8190	-12.3430
4th Resonant Frequency (1595.6997 Hz)	-13.5426	3.6849	33.9960
5th Resonant Frequency (2406.4086 Hz)	-26.8545	-17.6537	5.0026
6th Resonant Frequency (3388.6949 Hz)	-12.1291	1.7440	5.9022
7th Resonant Frequency (4477.8042 Hz)	-26.9088	-25.1462	-20.4433
8th Resonant Frequency (6483.6948 Hz)	8.6214	19.4543	-9.0166
9th Resonant Frequency (8230.2249 Hz)	19.8599	34.2888	9.4481
Summation	-226.7073	25.6377	45.2379

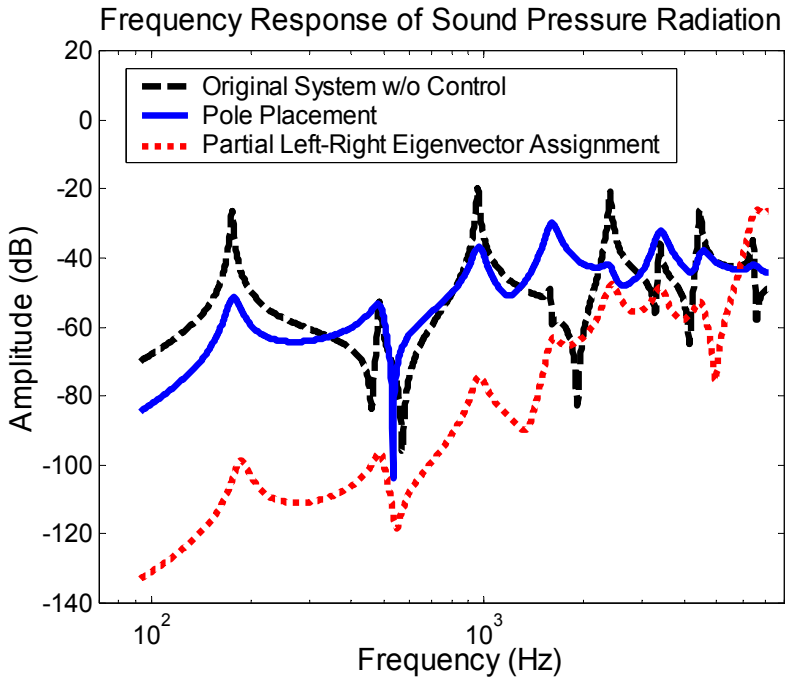

Figure 5-7: Frequency response of sound pressure radiation at the microphone receiver (assigned left eigenvectors: 1st mode; assigned right eigenvectors: other modes).

Figure **5-7** shows the frequency response of the sound pressure radiation at the microphone receiver by the pole placement and partial left-right eigenvector assignment methods, respectively. The closed-loop eigenvalues with the two methods are set to be the same so that one can fairly evaluate the further improvement achieved mainly by eigenvector assignment. In the partial left-right eigenvector assignment case, the left eigenvectors corresponding to the 1st mode (the eigenvalues are -44.013≤1106.881i) are first assigned and then the right eigenvectors at the remaining modes are assigned in the second step. It shows that through the partial left-right eigenvector assignment approach,

the structural noise can be further reduced significantly throughout the broad frequency range including the first 7 resonant frequencies.

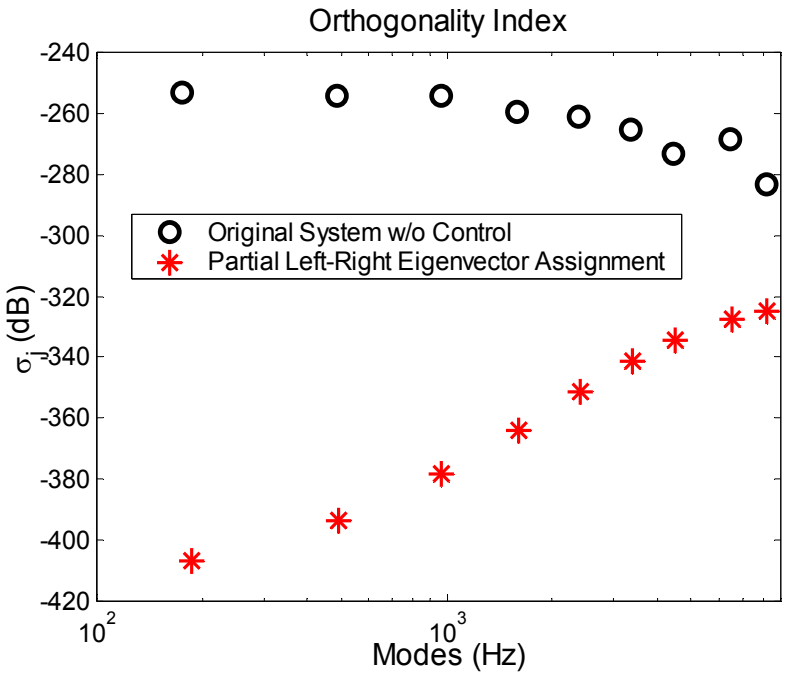

Figure **5-8**: Orthogonality indices w/ and w/o partial left-right eigenvector assignment (assigned left eigenvectors: 1st mode)

Figure **5-8** shows the orthogonality indices of selected modes with and without the partial left-right eigenvector assignment method. With the partial left-right eigenvector assignment method, the orthogonality indices can be reduced, that means the system capability of disturbance rejection can be enhanced by this method. It is also noted that the orthogonality index at the first mode is significantly suppressed because the left eigenvectors at this mode have been assigned exactly.

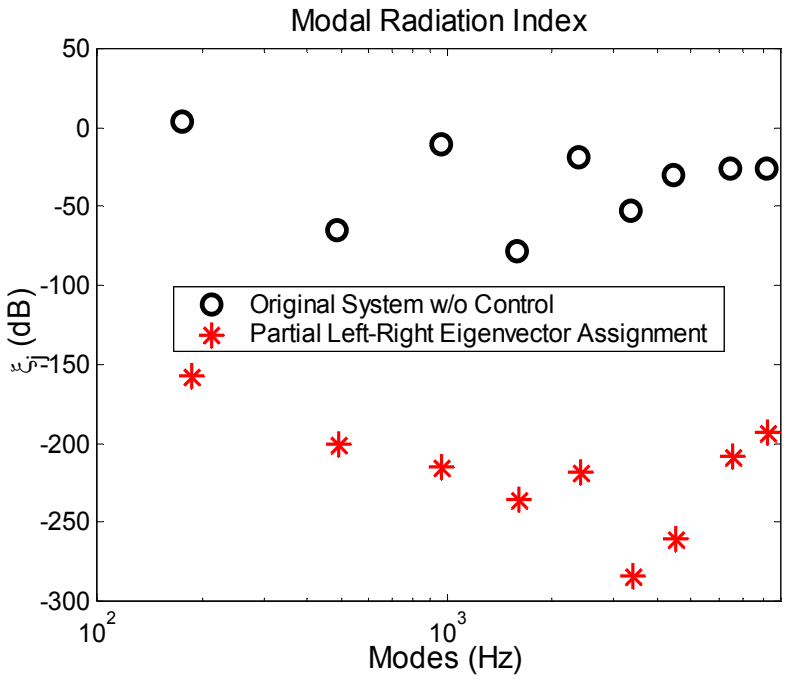

Figure 5-9: Modal radiation indices w/ and w/o partial left-right eigenvector assignment (assigned right eigenvectors: other mode except to 1st mode)

Figure **5-9** shows the modal radiation indices of selected modes with and without the partial left-right eigenvector assignment method. It shows that the modal radiation indices can be reduced by the partial left-right eigenvector assignment. From the analysis in Figure **5-8** and Figure **5-9**, one can conclude that the proposed approach can achieve both disturbance rejection and modal velocity distribution tailoring, therefore, the structural sound pressure radiation can be suppressed.

5.5 Summary

Both the simultaneous left-right eigenvector assignment and partial left-right eigenvector assignment methods are applied for the active control of structural acoustic radiation. A new design criterion of right eigenvectors for structural noise control is derived. The desired right eigenvectors are determined by minimizing the modal radiation indices that quantify the radiation from modal velocity distribution. The desired left eigenvectors are selected to achieve disturbance rejection through the same procedures as in Chapter 2 and Chapter 3. Through numerical simulations on a clamped-clamped beam structure example, it is shown that the left-right eigenvector assignment methods can successfully achieve disturbance rejection and modal velocity tailoring, and thus can effectively reduce structural sound radiation.

Chapter 6

CONCLUSIONS AND RECOMMENDATIONS

6.1 Summary of Research Effort and Achievements

In this research, two left-right eigenvector assignment approaches are explored and investigated for active control of structural vibration and acoustic radiation, namely the simultaneous left-right eigenvector assignment method and the partial left-right eigenvector assignment method.

As discussed in Chapter 2, the simultaneous left-right eigenvector assignment algorithm is developed for structural vibration control, such that disturbance rejection and modal confinement can be achieved. A new formulation to select the desired left eigenvectors is developed. The desired closed-loop left eigenvectors can be determined through minimizing the orthogonality indices by solving a generalized eigenvalue problem. The analysis of the modal energy distribution and orthogonality index is proposed for providing insight. The effectiveness of the proposed method is demonstrated on a clamped-clamped beam structure example through numerical simulations. Conclusively, this approach can successfully achieve both disturbance

rejection and modal confinement concurrently, and thus can successfully achieve vibration suppression in the concerned region of the beam structure.

In Chapter 3, the partial left-right eigenvector assignment method is discussed. With this approach, the selected left and right eigenvectors are derived from the achievable subspaces and can be exactly assigned without approximation errors. The desired left eigenvectors are determined by minimizing the orthogonality indices. Reciprocally, the desired right eigenvectors are determined by minimizing the modal energy ratios based on the Rayleigh Principle. By assigning both the left and right eigenvectors with these strategies, this method can also satisfy both the disturbance rejection and modal confinement requirements for structural vibration control. The numerical simulation performed on a clamped-clamped beam structure test bed demonstrated the effectiveness of the method. The analysis results of the orthogonality indices and modal energy distribution show that this approach can enhance the system capability of disturbance rejection and re-distribute the modal energy concurrently, and thus the vibration amplitude in the concerned region of the beam structure can be significantly suppressed.

In Chapter 4, experimental efforts for structural vibration control utilizing the proposed left-right eigenvector assignment ideas are reported. The test results show that the measured vibration amplitude can be reduced through either the simultaneous left-right eigenvector assignment method or the partial left-right eigenvector assignment method.

In Chapter 5, the concept of left-right eigenvector assignment is expanded for structural acoustic radiation control. In this case, the desired right eigenvectors are re-

shaped by minimizing the modal radiation indices through solving a generalized eigenvalue problem. The design strategy of left eigenvectors is the same as for vibration control, in which the disturbance rejection ability is enhanced. Through numerical simulations on a clamped-clamped beam structure, the analysis result illustrates the effectiveness of proposed methods.

In general, it is difficult to conclude from the presented examples which of the two methods (the simultaneous left-right eigenvector assignment approach and the partial left-right eigenvector assignment method) will have better performance. In other words, the control performance with different methods is case-dependent. In the simultaneous left-right eigenvector assignment approach, all the left and right eigenvectors are assigned by closest approximation to the designer's wish. However, to achieve a satisfactory control performance, significant computation effort may be required to decide the weighting factors. Alternatively, only selected eigenvectors can be exactly assigned in the partial left-right eigenvector assignment method, however, satisfactory system performance can be obtained among a limited number of assignable combinations, in which the computation is more efficient as compared to the simultaneous left-right eigenvector assignment approach.

6.2 Recommendations for Future Work

In this thesis, the left-right eigenvector assignment methods are investigated and are shown to be promising for structural vibration and acoustic control. Extending from

the current effort, there are several interesting topics that could be further explored in the future, as discussed in the following sections.

6.2.1 Simultaneous Suppression on Structural Vibration and Acoustic Radiation

The first recommendation for future study is to develop a methodology that will take into account both the vibration and noise suppression performance. It has been shown that significant suppressions in vibration levels do not necessarily imply significant reductions in radiated sound pressure levels (Baumann et al., **1991**; Baumann et al., **1992**; Dehandschutter et al., **1999**). Therefore the control laws for structural vibration and acoustic control are developed separately in this thesis because the design strategies of mode shape tailoring are different for vibration suppression and noise reduction purposes. However, many industrial applications need low vibration amplitude and noise radiation concurrently. The suggested research idea is to investigate the feasibility of utilizing the optimization technique to develop the design law that will simultaneously consider the performance of vibration suppression and noise reduction.

6.2.2 Response Enhancement of Structural Vibration and Acoustic Radiation

This recommendation is to investigate the feasibility of utilizing the opposite concept of vibration and acoustics suppression for some engineering applications. Due to the physical meanings of the left and right eigenvectors, it is intuitively reasonable to explore the possibility of using the eigenvector assignment approach for enhancing the

frequency response in specific applications, such as sub-woofer, high-frequency loudspeaker or ultrasonic motor. Similarly to the concept of disturbance rejection, the left eigenvector can also be altered so that the control input authority is increased. Correspondently, the right eigenvectors can be tailored into strong-efficient modes at certain resonant frequencies so that the radiations from the mode shapes will be amplified. By properly assigning left and right eigenvectors, the structural response at certain frequency range can be enhanced.

6.2.3 Optimization of the Number and Location of Sensor/Actuator for Structural Vibration and Acoustic Control

Although effective left-right eigenvector assignment strategies have been developed in this thesis, they are synthesized for fixed sensor-actuator configurations. On the other hand, the selection of the number and locations of sensors and actuators is still a challenge. These factors will affect the system dynamics and may be critical to the control performance. As in many previous studies done in this field, the selection of performance index and objective function for optimizing the transducer distribution is still an important topic worth investigating in the future.

Bibliography

Andry, A. N. Jr., Shapiro, E. Y. and Chung, J. C., "Eigenstructure assignment for linear systems," *IEEE Transactions on Aerospace and Electronic Systems*, AES-19(5), pp.711-729, 1983.

Bai, M. R. and Wu, T. Y., "Study of the Acoustic Feedback Problem of Active Noise Control by Using the ℓ_1 and ℓ_2 Vector Space Optimization Approaches," *Journal of Acoustical Society of America*, Vol. 102, No. 2, pp. 1004-1012, 1997.

Bai, M. R. and Wu, T. Y., "Simulations of an internal model-based active noise control system for suppressing periodic disturbances," *ASME Journal of Vibration and Acoustics*, vol. 120 (1), pp. 111-116, 1998.

Balas, M. J., "Direct velocity feedback control of large space structures," *Journal of Guidance, Control, and Dynamics*, Vol. 2, No. 3, pp. 252-253, 1979.

Baumann, W. T., Saunders, W. R., and Robertshaw, H. H., "Active Suppression of Acoustic Radiation from Impulsively Excited Structures," *Journal of Acoustical Society of America*, Vol. 90, No. 6, pp. 3202-3208, 1991.

Baumann, W. T., Ho, F. S., and Robertshaw, H. H., "Active Structural Acoustic Control of Broadband Disturbances," *Journal of Acoustical Society of America*, Vol. 92, No. 4, pp. 1998-2005, 1992.

Blackstock, D. T., *Fundamentals of Physical Acoustics*, John Wiley & Sons, New York, 2000.

Burrows, S. P. and Patton, R. J., "Design of low-sensitivity modalized observers using left eigenvector assignment," *Journal of Guidance, Control, and Dynamics*, vol. 15 (3), pp. 779-782, 1992.

Chen, C. T., *Linear System Theory and Design*, Holt, Rinehart, and Winston, 1984.

Choi, J. W., Lee, J. G. and Kim, Y., "Design of an effective controller via disturbance accommodating left eigenstructure assignment," *Journal of Guidance , Control, and Dynamics*, Vol. 18, No. 2, pp. 347-354, 1995.

Choi, J. W., "A simultaneous assignment methodology of right/left eigenstructures," *IEEE Transactions on Aerospace and Electronic Systems*, Vol. 34, No. 2, pp.625-634, 1998.

Choura, S., "Control of flexible structures with the confinement of vibrations," *ASME Journal of Dynamic Systems, Measurement, and Control*, vol. 117 (2), pp. 155-164, 1995.

Choura, S. and Yigit, A. S., "Vibration confinement in flexible structures by distributed feedback," *Computers and Structures*, vol. 54 (3), pp. 531-540, 1995.

Clark, R. L. and Fuller, C. R., "Experiments on Active Control of Structurally radiated Sound Using Multiple Piezoelectric Actuators," *Journal of Acoustical Society of America*, Vol. 91, pp. 3313-3320, 1992.

Clarke T., Griffin S. J. and Ensor J., "Output feedback eigenstructure assignment using a new reduced orthogonality condition," *International Journal of Control*, vol. 76, no. 4, pp. 390-402, 2003.

Constans, E. W., Koopmann, G. H. and Belegundu, A. D., "The Use of Modal Tailoring to Minimize the Radiated Sound Power of Vibrating Shells: Theory and Experiment," *Journal of Sound and Vibration*, Vol. 217, No. 2, pp. 335-350, 1998.

Corr, L. R. and Clark, W. W. "Active and passive vibration confinement using piezoelectric transducers and dynamic vibration absorbers," *Proceedings of SPIE,* vol. 3668, pp.747-758, 1995.

Cunningham, T. B. "Eigenspace selection procedures for closed-loop response shaping with modal control," *Proceedings of the American Control Conference*, pp.178-186, 1980.

Davison, E. and Wang, S., "On pole assignment in linear multivariable systems using output feedback," *IEEE Transactions on Automatic Control*, vol. 20, pp. 516-518, 1975.

Dehandschutter, W. and Henrioulle, K., Swevers, J., and Sas, P., "Model-Based Feedback Control of Acoustic Radiation from Vibrating Structures by Means of Structural Control," *Flow, Turbulence, and Combustion*, Vol. 61, No. 1, pp. 239-254, 1999.

Elliott, S. J. and Johnson, M. E., "Radiation Modes and the active Control of Sound Power," *Journal of Acoustical Society of America*, Vol. 94, No. 4, pp. 2194-2204, 1993.

Fahmy, M. M. and O'Reilly, J., "Multistage parametric eigenstructure assignment by output-feedback control," *International Journal of Control*, vol. 48 (1), pp. 97-116, 1988.

Fletcher, L. R., "An intermediate algorithm for pole placement by output feedback in linear multivariable system," *International Journal of Control*, vol. 31 (6), pp. 1121-1136, 1980.

Fuller, C. R., "Active Control of Sound Transmission/Radiation from Elastic Plates by Vibration Inputs: I. Analysis," *Journal of Sound and Vibration*, Vol. 136, No. 1, pp. 1-15, 1990.

Fuller, C. R. and Burdisso, R. A., " A Wave Number Domain Approach to Active Control of Structure-borne Sound," *Journal of Sound and Vibration*, Vol. 148, pp. 335-360, 1991.

Fuller, C. R., Rogers, C. A. and Robertshaw, H. H., "Control of sound radiation with active/adaptive structures," *Journal of Sound and Vibration*, Vol. 157, No. 1, pp. 19-39, 1992.

Fuller, C. R. and von Flotow, A. H., "Active Control of Sound and Vibration," *IEEE Control Systems Magazine*, 9-19, 1995.

"IEEE Standard on Piezoelectricity," *ANSI/IEEE Std* 176-1987.

Klema, V. C. and Laub, A. J. "The singular value decomposition: its computation and some applications," *IEEE Transactions on Automatic Control*, AC-25(2), pp.164-176, 1980.

Konstanzer, P. and Kroeplin, B., "Performance considerations in the control of helicopter vibration," *Proceedings of SPIE*, vol. 3667, pp. 462-473, 1999.

Kwakernaak, H. and Sivan, R., *Linear Optimal Control Systems*, Wiley, New York, 1972.

Kwon, B. H. and Youn, M. J. "Eigenvalue-generalized eigenvector assignment by output feedback," *IEEE Transactions on Automatic Control*, AC-32(5), pp.417-421, 1987.

Lee, H. -K. and Park, Y. -S., "A Near-Field Approach to Active Control of Sound Radiation from A Fluid-Loaded Rectangular Plate," *Journal of Sound and Vibration*, Vol. 196, No. 5, pp. 579-593, 1996.

Li, P., Cheng, L., Li, Y. Y. and Chen, N., "Robust control of a vibrating plate using m– synthesis approach," *Thin-Walled Structure*, vol. 41 (11), pp. 973-986, 2003.

Ljung, L., *System Identification: Theory for the User*, Prentice Hall, 1999.

Maillard, J. P. and Fuller, C. R., "Active Control of Sound Radiation from Cylinders with Piezoelectric Actuators and Structural Acoustic Sensing," *Journal of Sound and Vibration*, Vol. 222, No. 3, pp. 363-388, 1999.

Meirovitch, L. *Computational Methods in Structural Dynamics*, Sijthoff & Noorhoff, 1980.

Meirovitch, L. and Thangjitham, S., "Active Control of Sound Radiation Pressure," *Journal of Vibration, Acoustics, Stress, and Reliability in Design*, Vol. 112, No. 2, pp. 237-244, 1990.

Meirovitch, L. and Thangjitham, S., "Control of Sound Radiation from Submerged Plates," *Journal of Acoustical Society of America*, Vol. 88, pp. 402-407, 1990.

Moore, B. C., "On the flexibility offered by state feedback in multi-variable systems beyond closed-loop eigenvalue assignment," *IEEE Transaction on Automatic Control*, AC-21(5), pp. 689-692, 1976.

Naghshineh, K. and Koopmann, G. H., "Active Control of Sound Power Using Acoustic Basis Functions as Surface Velocity Filters," *Journal of Acoustical Society of America*, Vol. 93, No. 5, pp. 2740-2752, 1993.

Naghshineh, K. and Koopmann, G. H., "An Active Control Strategy for Achieving Weak Radiator structures," *ASME Journal of Vibration and Acoustics*, Vol. 116, pp. 31-37, 1994.

Nelson, P. A. and Elliott, S. J., *Active Control of Sound*, Academic, New York, 1992.

Patton, R. J., Willcox, S. M. and Winter, S. J., "A parameter insensitive technique for aircraft sensor fault analysis," *Journal of Guidance, Control, and Dynamics*, vol. 10 (3), pp. 359-367, 1987.

Roppenecker, G. and O'Reilly, J., "Parametric output feedback controller design," *Automatica*, vol. 25 (2), pp. 259-265, 1989.

Shelley, F. J. and Clark, W. W. "Active mode localization in distributed parameter systems with consideration of limited actuator placement, part 1: theory," *ASME Journal of Vibration and Acoustics*, vol. 122, no. 2, pp. 160-164, 2000b.

Shelley, F. J. and Clark, W. W. "Active mode localization in distributed parameter systems with consideration of limited actuator placement, part 2: simulations and experiments," *ASME Journal of Vibration and Acoustics*, vol. 122, no. 2, pp. 165-168, 2000c.

Song, B. –K. and Jayasuriya, S., "Active vibration control using eigenvector assignment for mode localization," *Proceedings of the American Control Conference*, pp. 1020-1024, 1993.

Srinathkumar, S., "Eigenvalue/eigenvector assignment using output feedback," *IEEE Transactions on Automatic Control*, vol. 23, pp. 79-81, 1978.

Sung, C. C. and Jan, C. T., "Active Control of Structurally Radiated Sound from Plates," *Journal of Acoustical Society of America*, Vol. 102, No. 1, pp. 370-381, 1997.

Sung, C. C. and Chiu, C. Y., "The Implementation of Modal Estimation for Structural Acoustics Control," Smart Materials and Structures, Vol. 6, No. 5, pp. 592-600, 1997.

Tang, J. and Wang, K. W. "Vibration confinement via optimal eigenvector assignment and piezoelectric networks," *ASME Journal of Vibration and Acoustics*, vol. 126, n 1, pp. 27-36, 2004.

Wie, B., Liu, Q. and Byun, K. W., "Robust H ¶ control synthesis method and its application to benchmark problems," *Journal of Guidance, Control and dynamics*, vol. 15 (5), pp. 1140-1148, 1992.

Wu, T. Y. and Wang, K. W., "Vibration isolator design via energy confinement through eigenvector assignment and piezoelectric networking," *Proceedings of SPIE*, *Smart Structures and Materials*, Vol. 5386, pp. 11-25, 2004.

Zhang, Q., Slater, G. L. and Allemang, R. J., "Suppression of undesired inputs of linear systems by eigenspace assignment," *Journal of Guidance , Control, and Dynamics*, Vol. 13, No. 3, pp. 330-336, 1990.

Appendix A

ANALYTICAL MODEL DERIVATION

A.1 Constitutive Equation of Piezoelectric Material

For one-dimensional structures with uni-axial loading, the constitutive relation of piezoelectric materials is (IEEE, **1987**)

$$\begin{Bmatrix} \tau_j \\ E_j \end{Bmatrix} = \begin{bmatrix} E_p & -h_{31} \\ -h_{31} & \beta_{33} \end{bmatrix} \begin{Bmatrix} \varepsilon_j \\ D_j \end{Bmatrix} \tag{A.1}$$

where t_j, $\P_j$, D_j and E_j represent the stress, strain, electrical displacement (charge/area) and electrical field (voltage/length along the transverse direction) within the j-th piezoelectric patch.

A.2 Integrated System of Beam Structure with Piezoelectric Actuator

The mathematical model of integrated system of beam structure with piezoelectric actuator referenced in Chapter 2 and Chapter 3 is derived as the following. The equations of motion are derived using extended Hamilton's principle.

$$\int_{t_1}^{t_2} \left(\delta T_{beam} + \delta T_{PZT} - \delta V_{beam} - \delta V T_{PZT} + \delta W \right) dt = 0 \tag{A.2}$$

The kinetic energy (T), potential energy (V) and virtual work ($\mathrm{d}W$) terms for the beam and piezoelectric patches are shown in Equation **A.3**.

$$\begin{aligned}
T_{beam} &= \frac{1}{2} \int_{volume} (\rho_r (\frac{\partial w}{\partial t})^2)_{beam} dV \\
T_{PZT} &= \frac{1}{2} \int_{volume} (\rho_p (\frac{\partial w}{\partial t})^2)_{PZT} dV \\
V_{beam} &= \frac{1}{2} \int_{volume} (\tau \varepsilon)_{beam} dV \\
V_{beam} &= \frac{1}{2} \int_{volume} (\tau \varepsilon + E_j D_j)_{beam} dV \\
\delta W &= f(t) \delta w_N
\end{aligned} \tag{A.3}$$

where w is the transverse displacement. The equations for beam bending with piezoelectric actuators thus are

$$\rho_b \frac{\partial^2 w}{\partial t^2} + \sum_{j=1}^{4} \rho_p \frac{\partial^2 w}{\partial t^2}(H(x-x_j^e) - H(x-x_j^s)) + c_d \frac{\partial w}{\partial t} + \frac{\partial^2}{\partial x^2}(E_b I_{beam} \frac{\partial^2 w}{\partial x^2})$$
$$+ \sum_{j=1}^{4} [\frac{\partial^2}{\partial x^2}(E_p I_{PZT} \frac{\partial^2 w}{\partial x^2}) + \frac{1}{2} h_{31} J_p \frac{\partial^2 D_i}{\partial x^2}](H(x-x_j^e) - H(x-x_j^s))$$
$$+ \sum_{j=1}^{4} \left[2E_p I_{PZT} \frac{\partial^3 w}{\partial x^3} + h_{31} J_p \frac{\partial D_i}{\partial x} \right](\delta(x-x_j^e) - \delta(x-x_j^s)) \qquad \text{(A.4)}$$
$$+ \sum_{j=1}^{4} \left[E_p I_{PZT} \frac{\partial^2 w}{\partial x^2} + \frac{1}{2} h_{31} J_p \frac{\partial D_i}{\partial x} \right](\delta'(x-x_j^e) - \delta'(x-x_j^s)) = f(t)$$
$$[\frac{\beta_{33} t_p}{w_p (x_j^e - x_j^s)} Q_j + \frac{h_{31} J_p}{w_p} \frac{\partial^2 w}{\partial x^2}](H(x-x_j^e) - H(x-x_j^s)) = V_j; \quad j = 1,..,4$$

where $x_j^e - x_j^s$ represents the length of *j*th piezoelectric patch, *H*(//) is the Heavidide's function, and $J_p = \frac{w_p}{2}\left[\left(\frac{t_b}{2} + t_p\right)^2 - \left(\frac{t_b}{2}\right)^2\right]$. Equation **A.5** shows the terms for the element of the beam and piezoelectric patches by finite element method (FEM).

$$T_{beam}^{e}=\frac{1}{2}\dot{w}_e^T\left(\frac{\rho_b A_{beamj} l_j}{420}\begin{bmatrix}156 & 22l_j & 54 & -13l_j\\ 22l_j & 4l_j^2 & 13l_j & -3l_j^2\\ 54 & 13l_j & 156 & -22l_j\\ -13l_j & -3l_j^2 & -22l_j & 4l_j^2\end{bmatrix}\right)\dot{w}_e$$

$$T_{PZT}^{e}=\frac{1}{2}\dot{w}_e^T\left(\frac{\rho_p A_{PZTj} l_j}{420}\begin{bmatrix}156 & 22l_j & 54 & -13l_j\\ 22l_j & 4l_j^2 & 13l_j & -3l_j^2\\ 54 & 13l_j & 156 & -22l_j\\ -13l_j & -3l_j^2 & -22l_j & 4l_j^2\end{bmatrix}\right)\dot{w}_e$$

$$V_{beam}^{e}=\frac{1}{2}w_e^T\left(\frac{E_b I_{beamj}}{l_j^3}\begin{bmatrix}12 & 6l_j & -12 & 6l_j\\ 6l_j & 4l_j^2 & -6l_j & 2l_j^2\\ -12 & -6l_j & 12 & -6l_j\\ 6l_j & 2l_j^2 & -6l_j & 4l_j^2\end{bmatrix}\right)w_e \qquad \text{(A.5)}$$

$$V_{PZT}^{e}=\frac{1}{2}w_e^T\left(\frac{E_p I_{PZTj}}{l_j^3}\begin{bmatrix}12 & 6l_j & -12 & 6l_j\\ 6l_j & 4l_j^2 & -6l_j & 2l_j^2\\ -12 & -6l_j & 12 & -6l_j\\ 6l_j & 2l_j^2 & -6l_j & 4l_j^2\end{bmatrix}\right)w_e$$

$$+w_e^T Q_j\left(h_{31}J_p\begin{bmatrix}0\\ -1\\ 0\\ 1\end{bmatrix}\right)+\frac{1}{2}\frac{A_{PZTj}\beta_{33}}{w_p^2 l_j}Q_j^2$$

where A_{beamj}, A_{PZTj} represent the element area for beam and piezoelectric patch respectively and l_j is the length of the element. $w_e=[w_j, \theta_j, w_{j+1}, \theta_{j+1}]^T$ is the displacement and slope vector of the element. I_{beam} and I_{PZT} are moments of inertia of beam and piezoelectric patches, respectively.

VITA

Tian-Yau Wu

Tian-Yau Wu was born, growing and educated in Miao-Li City, Taiwan until junior high school age. Through three years of senior high school education in Taipei City, Taiwan, he passed the college entrance examination and was admitted into National Chiao-Tung University (NCTU) in 1990. He graduated with the degree of Bachelor of Science in Mechanical Engineering in 1994 and was concurrently admitted into the graduate study of mechanical engineering with honor of exempt examination for the top ten excellent undergraduate students.

He joined the Acoustics and Vibration Laboratory for his graduate research and study under the advice of Professor Minghsian Bai. In 1996, he received the degree of Master of Science in Mechanical Engineering with the dissertation, "*A DSP-Based Active Noise Control System in a Duct by Using ℓ_1 and ℓ_2 Vector Space Optimization Techniques*". After the graduate study in NCTU, he served in the Chinese Army for twenty two months as the Second Lieutenant Leader of Air-Defense Artillery Platoon.

After the compulsory military service, he was recruited as an associate researcher at the Industrial Technology Research Institute (ITRI) in Hsin-Chu County, Taiwan in 1998 for industrial controller development.

Beginning in 2001, he enrolled in the doctorate program of Mechanical Engineering, The Pennsylvania State University (PSU), and accepted the research assistant position in Dr. Kon-Well Wang's Structural Dynamics and Controls Laboratory (SDCL), Center for Acoustics and Vibration (CAV) at PSU. Under the mentoring of Dr. Kon-Well Wang, his research was focused on structural dynamics and system modeling, piezoelectric material based smart system, structural vibration and acoustic control. He has presented four papers at *ASME*, *SPIE* and *ICAST* conferences and submitted two journal papers on topics concerning vibration isolation design, structural vibration suppression and acoustic reduction.